Supporting information for

Exploring the Potential of Malononitrile Functionalized Donor-Acceptor Systems for Non-Volatile Memory Device Applications

Ramachandran Gokul[a], Ramesh Gayathri[a], Predhanekar Mohamed Imran[b], Nattamai S. P. Bhuvanesh[c], and Samuthira Nagarajan[*a]

[a] *Division of Organic Electronics,* Department of Chemistry, Central University of Tamil Nadu, Thiruvarur- 610 005, India, snagarajan@cutn.ac.in
[b] Department of Chemistry, Islamiah College, Vaniyambadi - 635 752, India
[c] Department of Chemistry, Texas A&M University, College Station, TX 77842, USA

Table of contents

1. Synthetic route for the targeted compounds

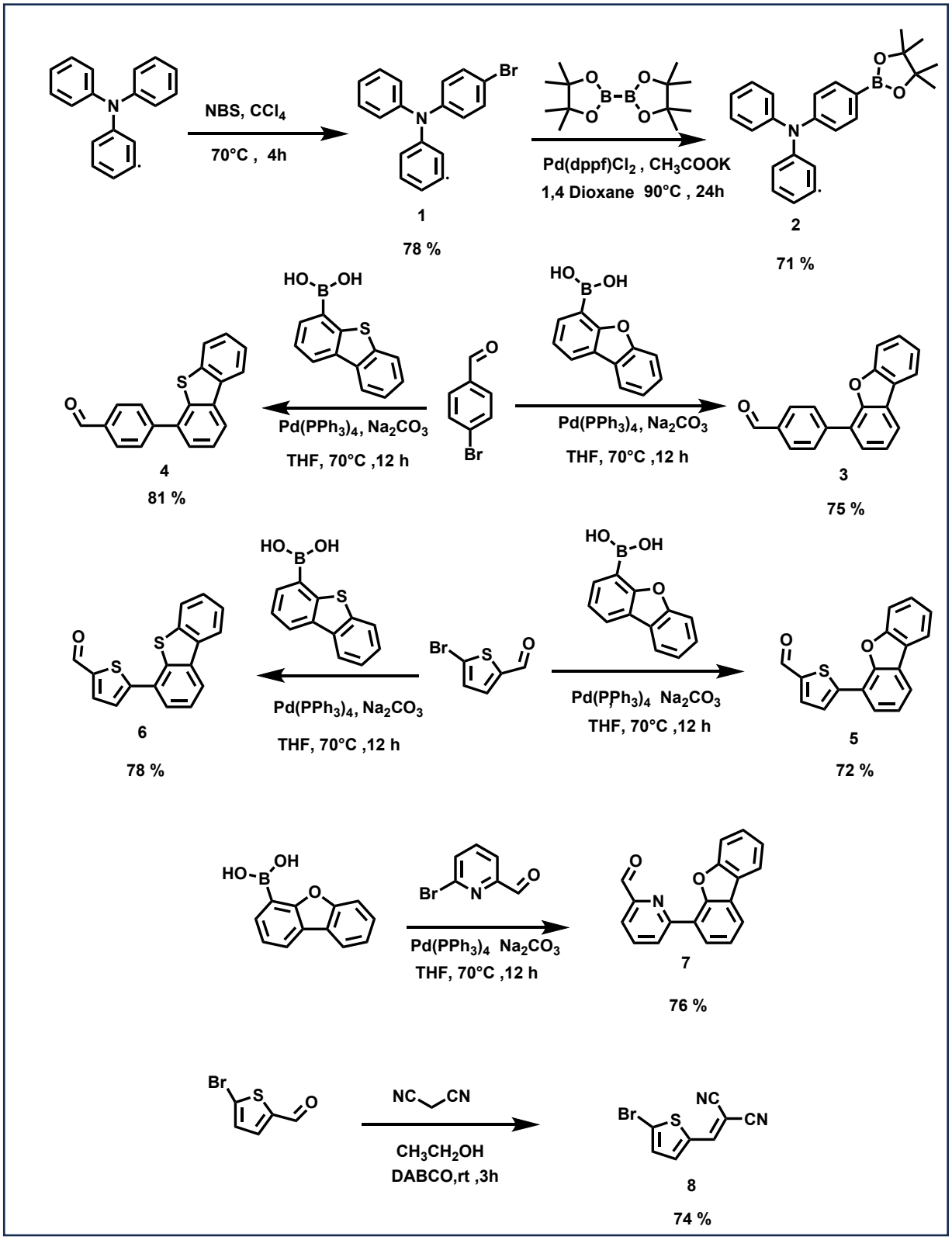

Scheme S1: Synthetic pathway of compounds 1-8

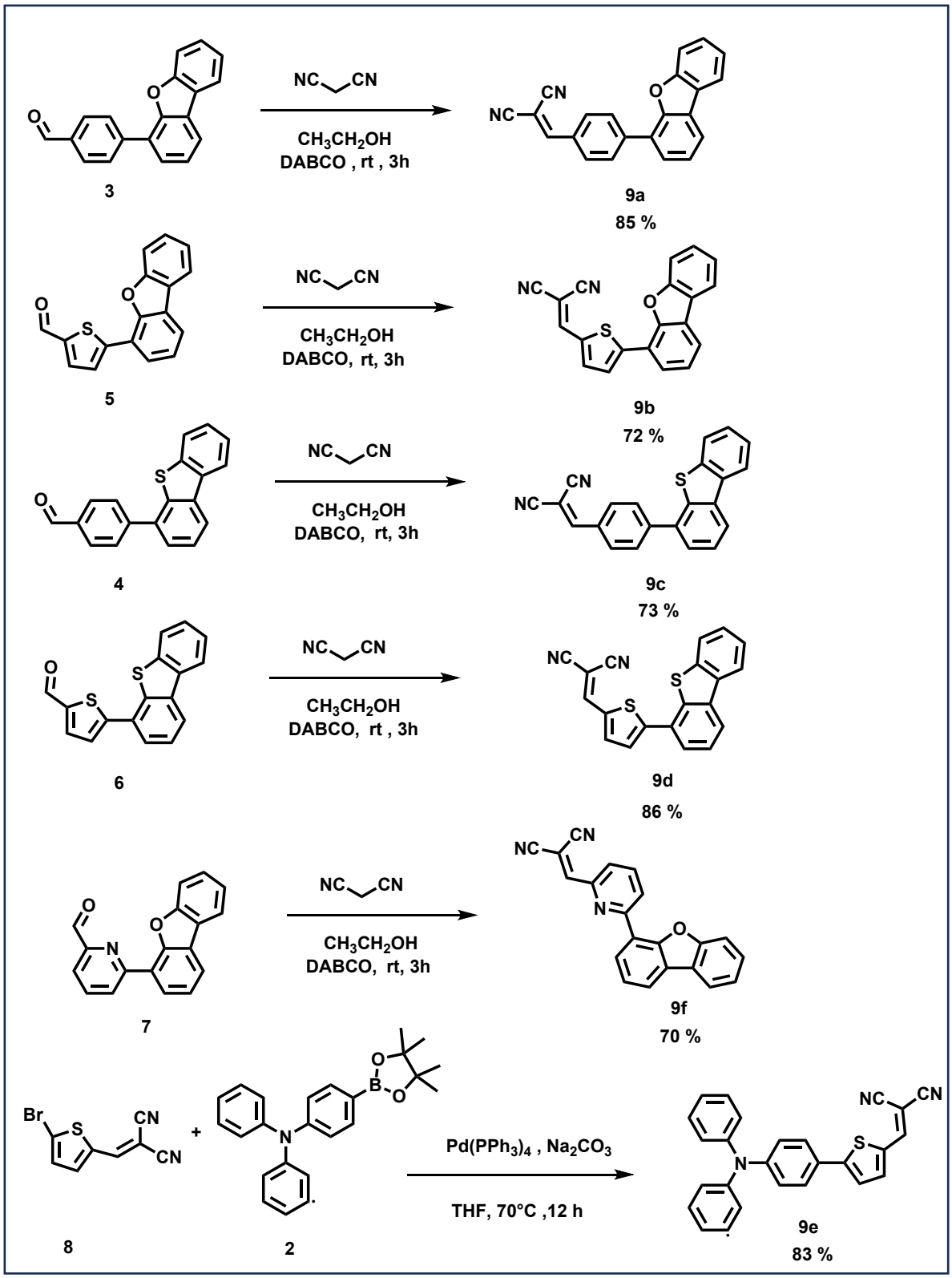

Scheme S2: Synthetic pathway of compounds 9a-f

2. Synthetic and analytical data of the targeted compounds

Compound 1: Triphenylamine (2g, 8.15 mmol) and NBS (1.450g, 8.15 mmol) were added in 20 mL of CCl_4 solvent taken in a 100 ml round bottom flask and refluxed at 80°C for 4 h. After cooling, the reaction mixture was filtered. Recrystallization of the residue from ethanol gave compound **1,** 78 % yield. ^{1}H NMR (400 MHz, $CDCl_3$) δ 7.34-7.30 (m, 2H), 7.27-7.23 (m, 4H), 7.08 – 7.01 (m, 6H), 6.95-6.93 (m, 2H). ^{13}C NMR (100 MHz, $CDCl_3$) δ 147.38, 147.03, 132.26, 129.39, 125.14, 124.42, 123.23, 114.76.

Compound 2: In a 100 mL two-necked round-bottom flask, compound **1**(1 g,3.09 mmol), bis(pinacolato)diborane (939.96 mg, 3.7 mmol), and potassium acetate (908.03 mg,9.25 mmol) were mixed with 20 mL of 1,4-dioxane. The mixture was degassed using N_2 before adding (22.51 mg 0.0308 mmol) of $PdCl_2$(dppf). It was then stirred overnight at 100°C in a nitrogen atmosphere. After completion, the reaction mixture was quenched with brine solution, and the organic layer was separated using dichloromethane (DCM). The solvent was removed under reduced pressure, and the residue was purified using column chromatography on silica gel (eluent: 99:1 hexane-ethyl acetate) to produce compound **2** in 71 % yield. ^{1}H NMR (400 MHz, $CDCl_3$) δ 7.67 (d, *J* = 8.4 Hz, 2H), 7.24 (m, 4H), 7.10 (d, *J* = 7.6 Hz, 4H), 7.04 – 7.02 (m, 4H), 1.33 (s, 12H). ^{13}C NMR (100 MHz, $CDCl_3$) δ 150.51, 147.43, 135.91, 129.35, 125.03, 123.66, 122.28, 83.60, 24.

General synthetic procedure for Suzuki Mayura coupling reaction: Brominated compound (1 eq) was dissolved in 30 mL tetrahydrofuran and placed in a two-neck round bottom flask. The solution was purged with nitrogen for 20 minutes. A catalytic amount of $Pd(PPh_3)_4$ (0.05 eq) was added and continued purging with nitrogen for another 15 minutes. A solution of 2 M Na_2CO_3 and appropriate arylboronic acid or boronic acid pinacol ester (1.3 eq) was added. The mixture was refluxed under inert conditions for 12 hours at 70 °C. After the completion of the reaction, the mixture was cooled and extracted using DCM. The residue was purified by column chromatography using a hexane/ethyl acetate solvent system.

Compound 3: As per the general procedure, 4-bromobenzaldehyde (1g,5.40 mmol) and dibenzo[b,d]furan-4-ylboronic acid (1.55g,7.02 mmol) were allowed to react to give compound **3**. The product was purified by column chromatography on silica (hexane-ethyl acetate 99:1) to give a white crystalline solid with a yield of 75 % .^{1}H NMR (400 MHz, $CDCl_3$) δ 10.11 (s, 1H), 8.11 (d, *J* = 8.3 Hz, 2H), 8.06 – 8.03 (m, 2H), 8.02 – 7.99 (m, 2H), 7.67 – 7.61 (m, 2H), 7.52 – 7.45 (m, 2H), 7.39 (t, *J* = 7.5 Hz, 1H). ^{13}C NMR (100 MHz, $CDCl_3$) δ 192.04,

156.13, 153.32, 142.63, 135.43, 130.14, 129.36, 127.57, 126.91, 125.27, 124.39, 123.93, 123.40, 123.07, 120.87, 111.90.

Compound 4: As per the general procedure,4-bromobenzaldehyde (1g, 5.40 mmol) and dibenzo[b,d]thiophene-4-ylboronic acid (1.6g,7.02 mmol) were allowed to react to give the product **4**. The product was purified by column chromatography on silica (hexane-ethyl acetate 99:2) to give a light-yellow solid with a yield of 81 %. ^{1}H NMR (400 MHz, $CDCl_3$) δ 10.11 (s, 1H), 8.23 – 8.19 (m, 2H), 8.06 – 8.03 (m, 2H), 7.95 – 7.91 (m, 2H), 7.86 – 7.82 (m, 1H), 7.59 (t, *J* = 7.6 Hz, 1H), 7.54 – 7.48 (m, 3H). ^{13}C NMR (100 MHz, $CDCl_3$) δ 191.80, 146.70, 139.34, 138.42, 136.56, 135.79, 135.62, 135.58, 130.27, 128.97, 127.07, 125.24, 124.63, 122.66, 121.83, 121.40

Compound 5: As per the general procedure, 5-bromothiophene-2-carbaldehyde (1g, 5.23 mmol) and dibenzo[b,d]furan-4-ylboronic acid (1.44g,6.8 mmol) were allowed to react to give the product **5**. The product was purified by column chromatography on silica (hexane-ethyl acetate 99:1) to give a white crystalline solid with a yield of 72 %. ^{1}H NMR (400 MHz, $CDCl_3$) δ 9.97 (s, 1H), 8.01 – 7.96 (m, 3H), 7.86 (s, 1H), 7.79 (dd, *J* = 7.7, 0.9 Hz, 1H), 7.68 (d, *J* = 8.3 Hz, 1H), 7.52 (dd, *J* = 15.6, 1.2 Hz, 1H), 7.40 (dd, *J* = 7.9, 5.8, 2H). ^{13}C NMR (100 MHz, $CDCl_3$) δ 183.10, 156.19, 152.37, 148.44, 142.60, 137.21, 127.82, 127.12 , 125.41, 123.64, 123.36, 121.52, 120.90, 118.03, 112.00.

Compound 6: As per the general procedure, 5-bromothiophene-2-carbaldehyde (1g,5.23 mmol) and dibenzo[b,d]thiophene-4-ylboronic acid (1.55g,6.8mmol) were allowed to react to give the product **6**. The product was purified by column chromatography on silica (hexane-ethyl acetate 99:1) to give a light-yellow solid with a yield of 78 %. ^{1}H NMR (400 MHz, $CDCl_3$) δ 9.97 (s, 1H), 8.26 – 8.16 (m, 2H), 7.91 – 7.87 (m, 1H), 7.85 (d, *J* = 3.9 Hz, 1H), 7.72 (dd, *J* = 5.0, 2.4 Hz, 2H), 7.57 – 7.49 (m, 3H). ^{13}C NMR (100 MHz, $CDCl_3$) δ 183.07, 152.28, 142.94, 139.14, 137.79, 137.02, 135.24, 128.49, 127.38, 126.96, 126.53, 125.17, 124.88, 122.71, 122.32, 121.87.

Compound 7: As per the general procedure, 6-bromopyridine aldehyde and dibenzo[b,d]furan-4-ylboronic acid were allowed to react to give the product **7**. The product was purified by column chromatography on silica (hexane-ethyl acetate 99:1) to give a white crystalline solid with a yield of 76 %. ^{1}H NMR (400 MHz, $CDCl_3$) δ 10.22 (s, 1H), 8.71 (d, *J* = 7.8 Hz, 1H), 8.47 (d, *J* = 7.7 Hz, 1H), 8.02 (dd, *J* = 26.3, 12.6, Hz, 4H), 7.66 (d, *J* = 8.2 Hz, 1H), 7.53 (dd, *J* = 12.6, 4.7 Hz, 2H), 7.40 (t, *J* = 7.5 Hz, 1H). ^{13}C NMR (100 MHz, $CDCl_3$) δ

194.02, 156.03, 154.23, 153.78, 152.74, 137.77, 128.34, 127.53, 127.24, 125.36, 123.85, 123.44, 123.21, 122.88, 122.03, 120.81, 120.06, 111.80

General procedure for Knoevenagel condensation reaction: Aldehyde (1 eq) was dissolved in 15 mL ethanol in a 50 mL round bottom flask. To this solution, (1 eq) of malononitrile followed by DABCO (0.1 equiv) was added as a catalyst. The mixture was stirred for 3 h. The precipitate was filtered, dried, and recrystallized from suitable solvents to get a pure product.

Compound 8: As per the general procedure, 5-bromothiophene-2-carbaldehyde was allowed to react with malononitrile to give the product **8**. The product was recrystallized using DCM to give a yellow crystalline solid with a yield of 74 %. ^{1}H NMR (400 MHz, $CDCl_3$) δ 7.75 (s, 1H), 7.50 (d, *J* = 4.0 Hz, 1H), 7.24 (d, *J* = 4.1 Hz, 1H). ^{13}C NMR (100 MHz, $CDCl_3$) δ 149.94, 138.72, 136.79, 131.92, 126.53, 113.51, 112.88, 78.73.

Compound 9a: As per the general procedure, compound **3** was allowed to react with malononitrile to give yellow solid compound **9a** with a yield of 85 %. ^{1}H NMR (400 MHz, $CDCl_3$) δ 8.15 (d, *J* = 8.6 Hz, 2H), 8.09 (d, *J* = 8.6 Hz, 2H), 8.03 (t, *J* = 7.5 Hz, 2H), 7.85 (s, 1H), 7.71 – 7.61 (m, 2H), 7.56 – 7.46 (m, 2H), 7.41 (t, *J* = 7.9 Hz, 1H). ^{13}C NMR (100 MHz, $CDCl_3$) δ 159.22, 156.16, 153.35, 142.92, 131.21, 130.05, 129.70, 127.72, 126.68, 125.47, 123.98, 123.51, 123.20 , 121.45 , 120.85, 113.92, 112.80, 111.89, 82.30. HRMS (ESI) (m/z): $C_{22}H_{12}N_2O$,Calc $[M]^+$: 320.0944, Observed $[M]^+$: 320.0965.

Compound 9b: As per the general procedure, compound **5** was allowed to react with malononitrile to give the compound **9b**. The product was recrystallized using chloroform to provide an orange solid with a yield of 72 %. ^{1}H NMR (400 MHz, $CDCl_3$) δ 8.10 (d, *J* = 4.2 Hz, 1H), 8.01 (dd, *J* = 7.5, 4.5 Hz, 2H), 7.87 (d, *J* = 3.8 Hz, 2H), 7.83 (d, *J* = 7.7 Hz, 1H), 7.69 (d, *J* = 8.2 Hz, 1H), 7.54 (t, *J* = 8.3 Hz, 1H), 7.43 (q, *J* = 7.5 Hz, 2H). ^{13}C NMR (100 MHz, $CDCl_3$) δ 156.37, 152.50 , 150.71, 139.45, 134.42, 127.84, 125.61, 123.69, 122.31, 120.96, 117.31, 114.22, 113.37, 112.04, 84.92. HRMS (ESI) (m/z): $C_{20}H_{10}N_2OS$, Calc $[M]^+$: 326.0508, Observed $[M]^+$: 326.0522.

Compound 9c: As per the general procedure, compound **4** was allowed to react with malononitrile to give an orange solid compound **9c** with a yield of 73 %. ^{1}H NMR (400 MHz, $CDCl_3$) δ 8.23 (d, *J* = 7.5 Hz, 1H), 8.21 (d, *J* = 5.0 Hz, 1H), 8.06 (t, *J* = 9.1 Hz, 2H), 7.98 – 7.90 (m, 2H), 7.89 – 7.82 (m, 2H), 7.62 – 7.58 (m, 1H), 7.51 (dd, *J* = 11.4, 5.0 Hz, 3H). ^{13}C NMR (100 MHz, $CDCl_3$) δ 159.13, 146.97, 139.18, 138.33, 136.74, 135.49, 134.86, 131.42,

130.35, 129.41, 129.01, 127.17, 125.40, 124.77, 122.68, 121.89, 82.67. HRMS (ESI) (m/z): $C_{22}H_{12}N_2S$, Calc $[M]^+$: 336.0715, Observed $[M]^+$: 336.0738.

Compound 9d: As per the general procedure, compound **6** was allowed to react with malononitrile to give orange solid compound **9d** with a yield of 86 %. ^{1}H NMR (400 MHz, $CDCl_3$) δ 8.24 (d, *J* = 7.2 Hz, 1H), 8.23 – 8.18 (m, 1H), 7.94 – 7.88 (m, 1H), 7.88 – 7.83 (m, 2H), 7.79 (dd, *J* = 8.3, 5.8 Hz, 2H), 7.62 – 7.51 (m, 3H). ^{13}C NMR (100 MHz, $CDCl_3$) δ 154.35, 150.53, 139.32, 137.81, 137.24, 135.10, 134.71, 127.57, 127.20, 126.96, 125.27, 125.06, 122.96,122.76, 121.92, 114.05, 113.21, 77.58. HRMS (ESI) (m/z): $C_{20}H_{10}N_2S_2$, Calc $[M]^+$: 342.0279, Observed $[M]^+$: 342.0299.

Compound 9e: As per the general procedure for the Suzuki coupling reaction, compounds **2** and **8** were allowed to react to give compound **9e**. The product was purified by column chromatography on silica (hexane-ethyl acetate 99:1) to provide a red crystalline solid yield of 70 %. ^{1}H NMR (400 MHz, $CDCl_3$) δ 7.75 (s, 1H), 7.68 (d, *J* = 4.1 Hz, 1H), 7.53 (d, *J* = 8.7 Hz, 2H), 7.34 – 7.29 (m, 5H), 7.13 (dd, *J* = 13.8, 7.5 Hz, 6H), 7.05 (d, *J* = 8.7 Hz, 2H). ^{13}C NMR (100 MHz, $CDCl_3$) δ 150.43, 149.80, 146.67, 140.54, 129.69, 127.59, 125.51, 124.91, 124.35, 123.28, 121.72, 113.74, 74.98. HRMS (ESI) (m/z): $C_{26}H_{17}N_3S$, Calc $[M]^+$: 403.1137, Observed $[M]^+$: 403.116.

Compound 9f: As per the general procedure, compound **7** was allowed to react with malononitrile to give compound **9f**. The product was recrystallized using an ether-DCM mixture to give a white crystalline solid with a yield of 83 %. ^{1}H NMR (400 MHz, $CDCl_3$) δ 8.85 (d, *J* = 7.7 Hz, 1H), 8.74 (dd, *J* = 7.8, 1.2 Hz, 1H), 8.09 – 8.00 (m, 3H), 7.66 (d, *J* = 8.2 Hz, 1H), 7.60 – 7.49 (m, 3H), 7.43 – 7.38 (m, 1H). ^{13}C NMR (100 MHz, $CDCl_3$) δ 157.14, 155.90, 155.28, 153.91, 148.25, 138.15, 128.26, 127.49, 126.03, 125.29, 123.78, 123.29, 122.67, 122.22 , 120.82 , 113.90, 112.72, 111.69, 86.76. HRMS (ESI) (m/z): $C_{22}H_{12}N_3O$, Calc $[M+H]^+$: 322.0975, Observed $[M+H]^+$: 322.0994.

3. ^{1}H, ^{13}C NMR, HRMS and IR spectra of the synthesized compounds

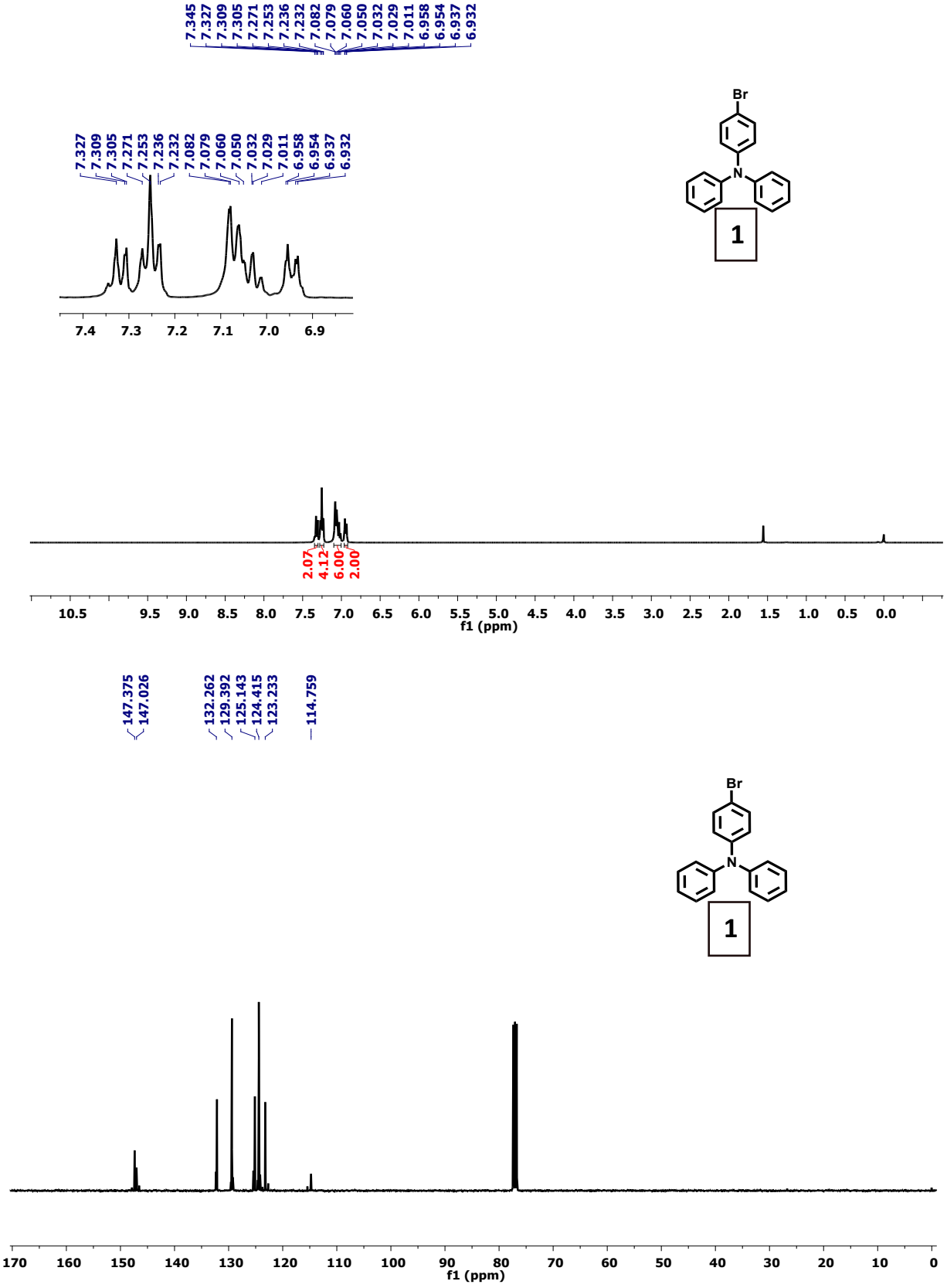

Figure S1: ^{1}H and ^{13}C NMR spectra of compound **1**

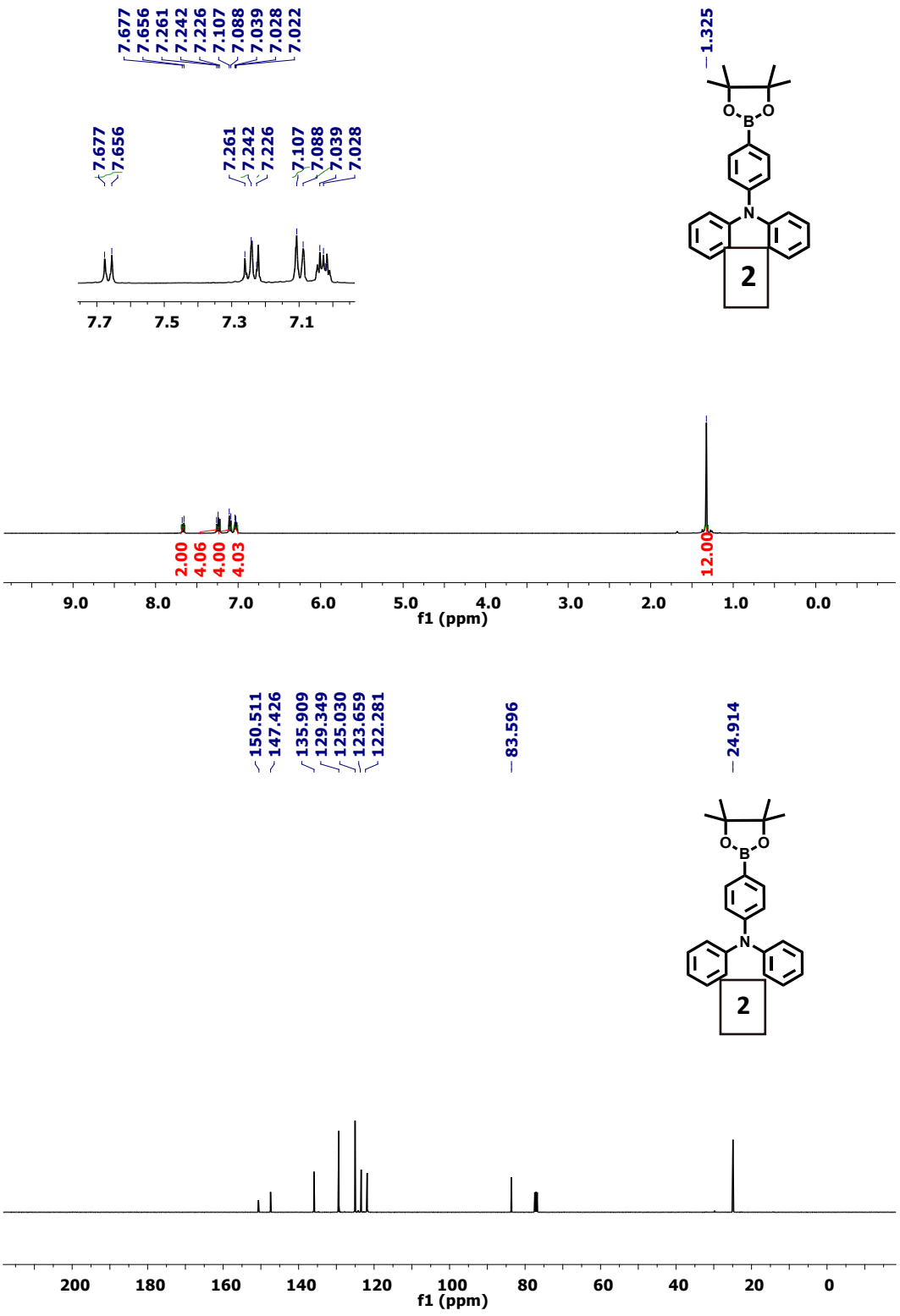

Figure S2: ^{1}H and ^{13}C NMR spectra of compound **2**

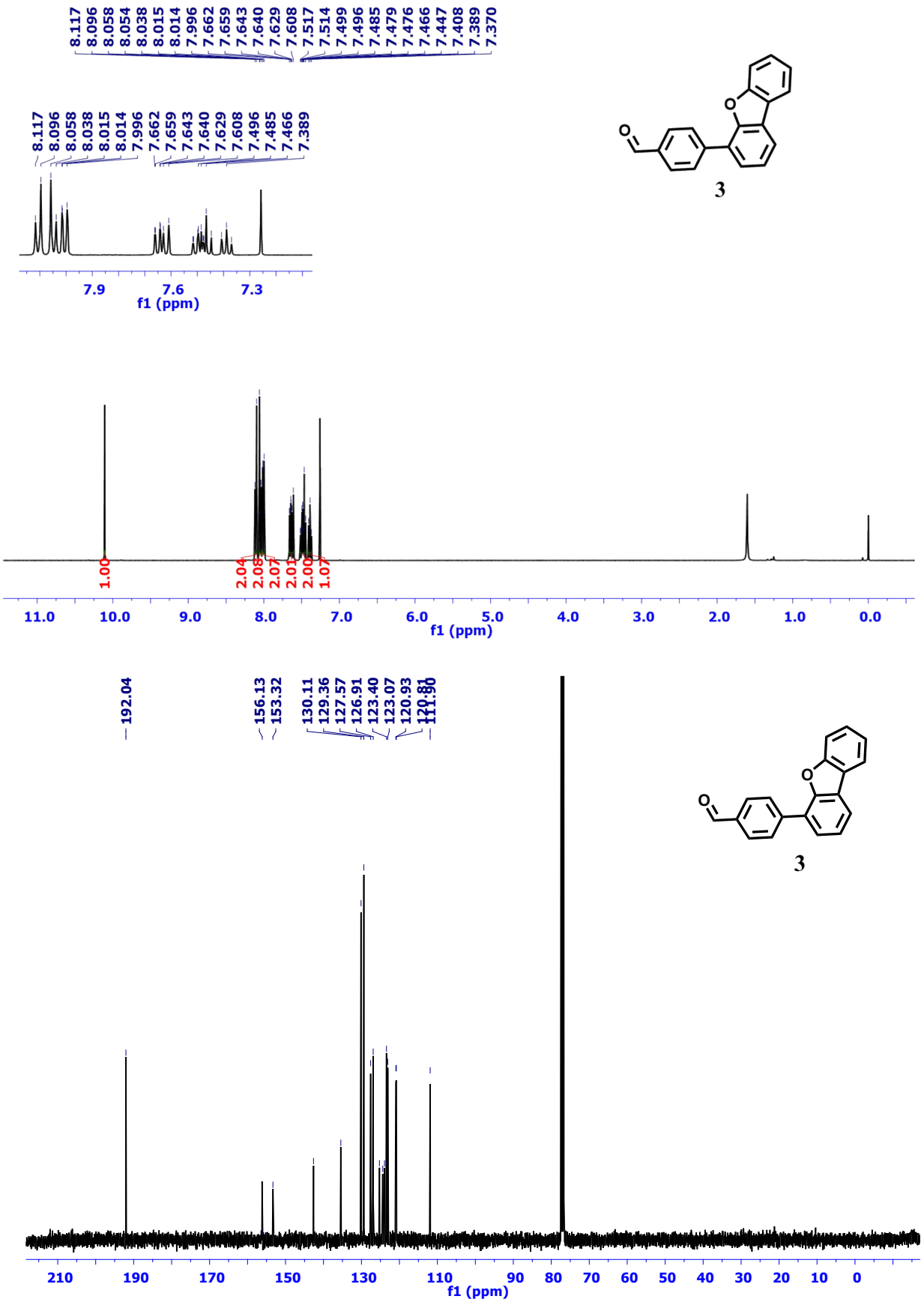

Figure S3 : ^{1}H and ^{13}C NMR spectra of compound **3**

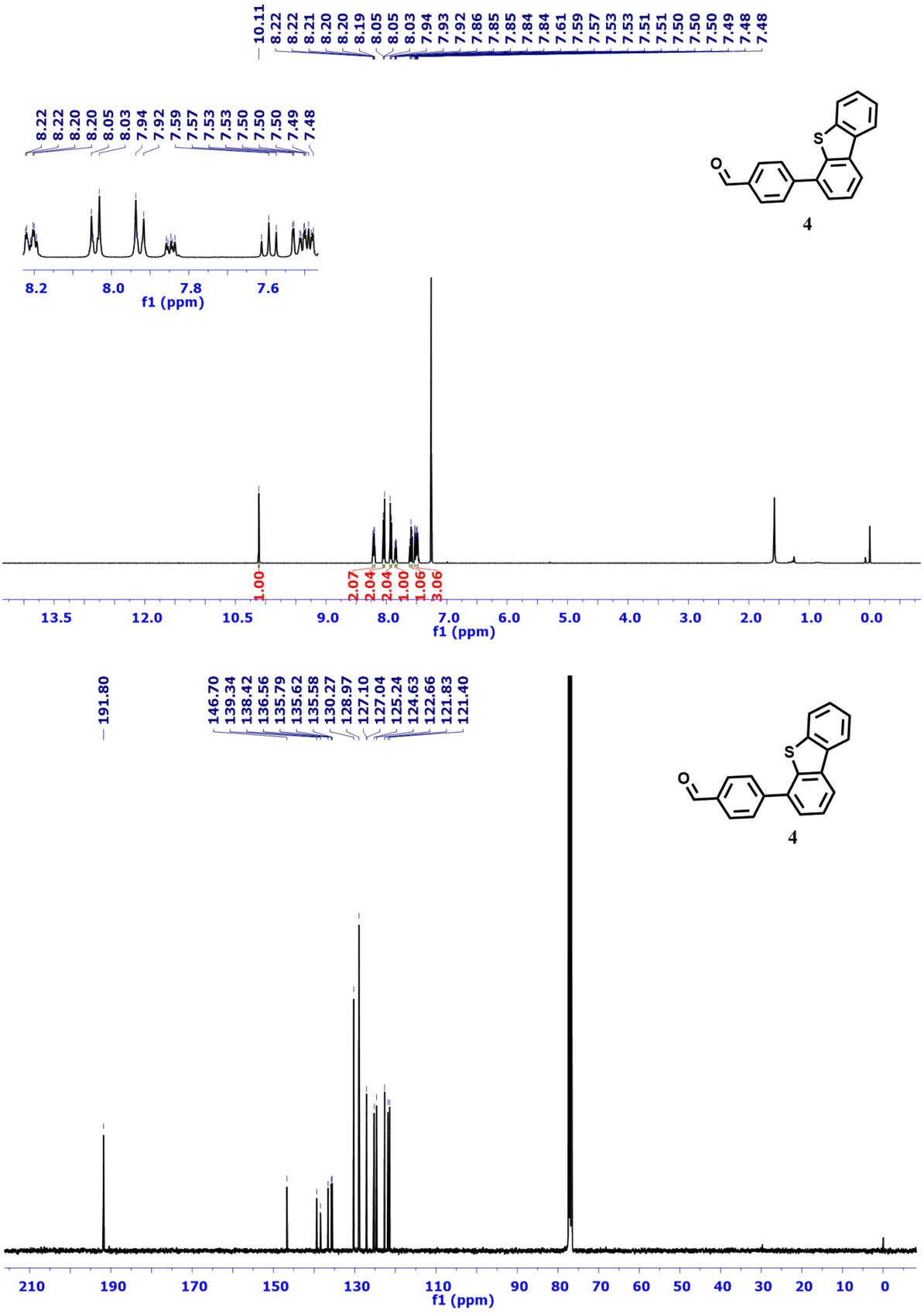

Figure S4: ^{1}H and ^{13}C NMR spectra of compound **4**

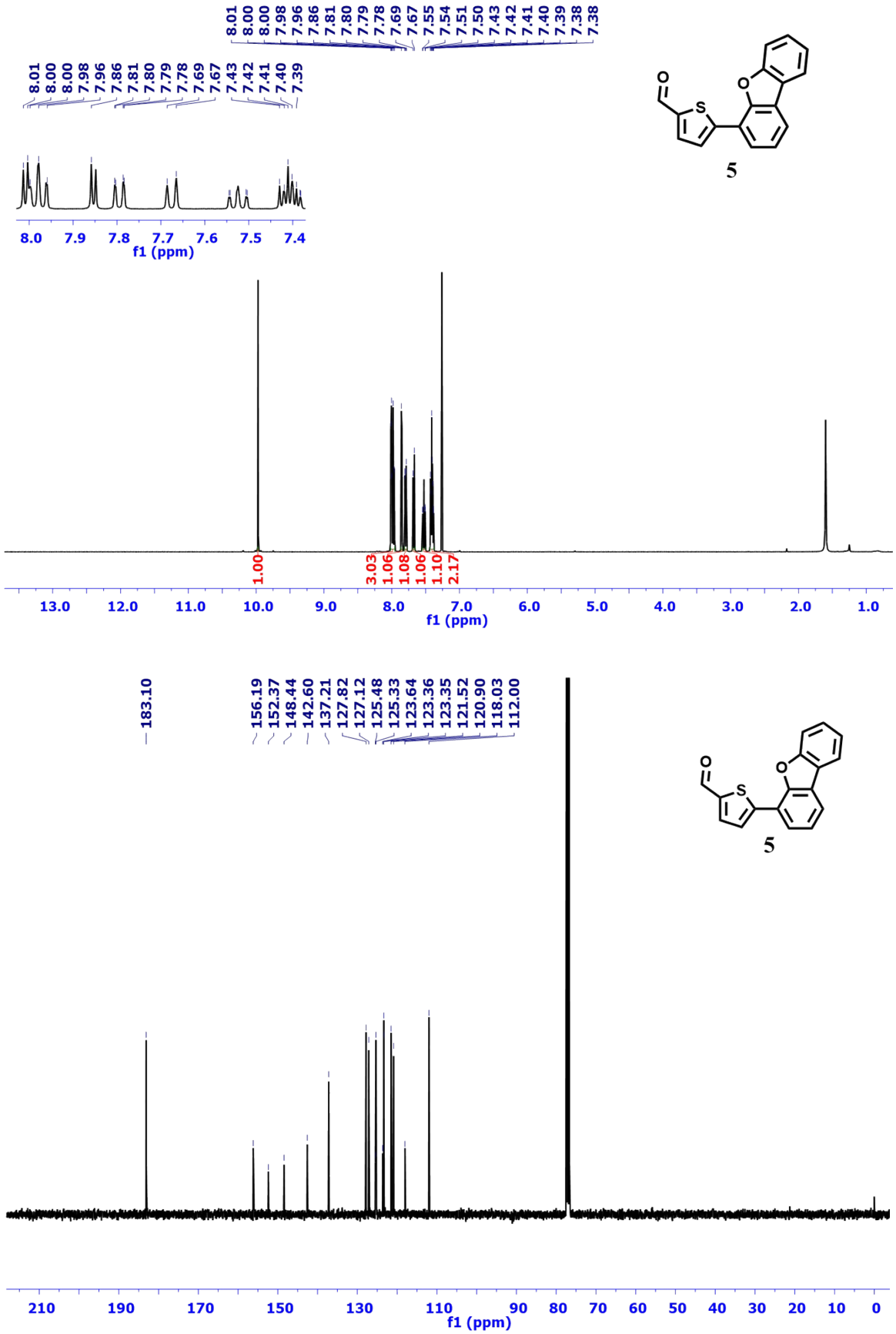

Figure S5: ^{1}H and ^{13}C NMR spectra of compound **5**

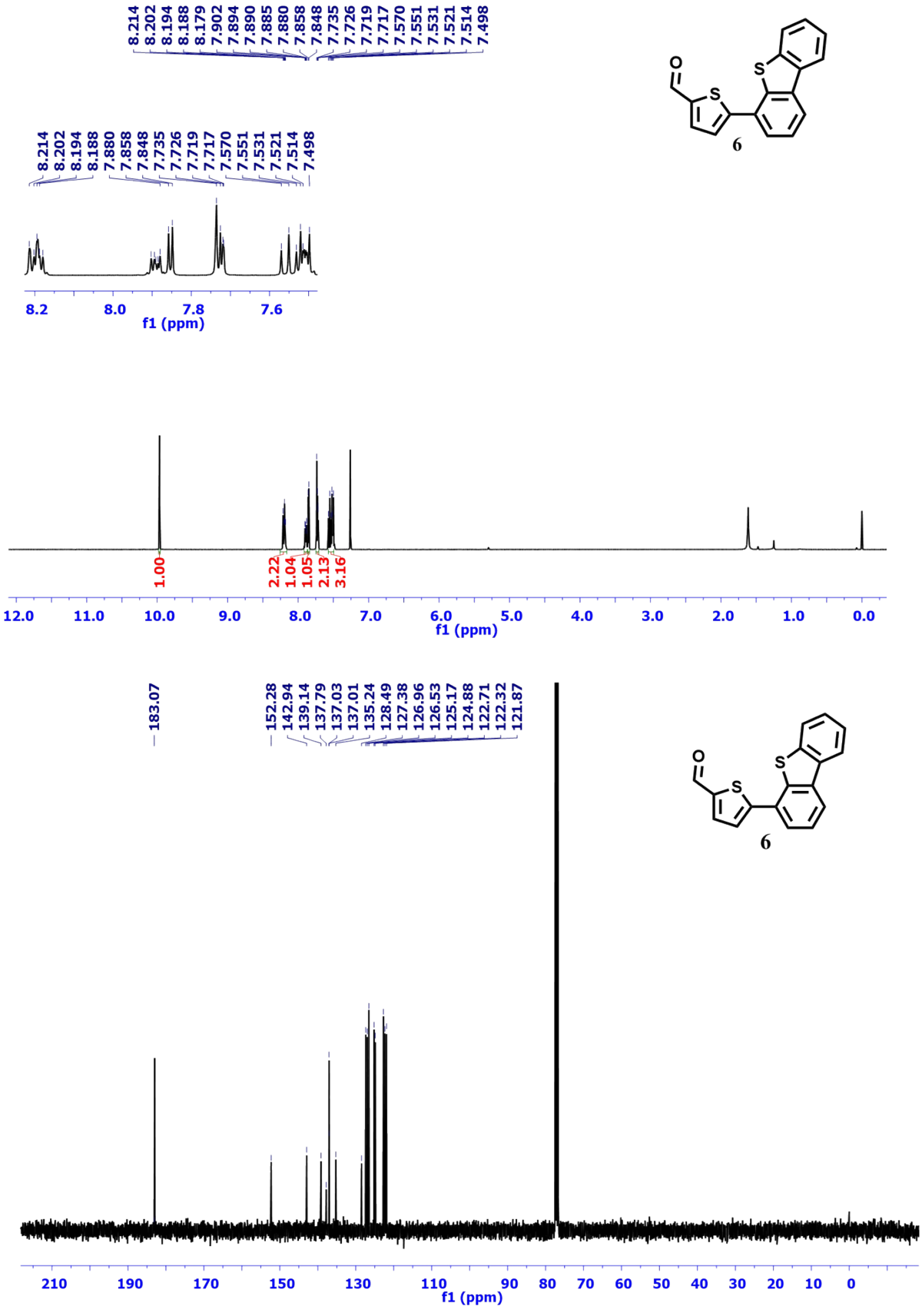

Figure S6: ^{1}H and ^{13}C NMR spectra of compound **6**

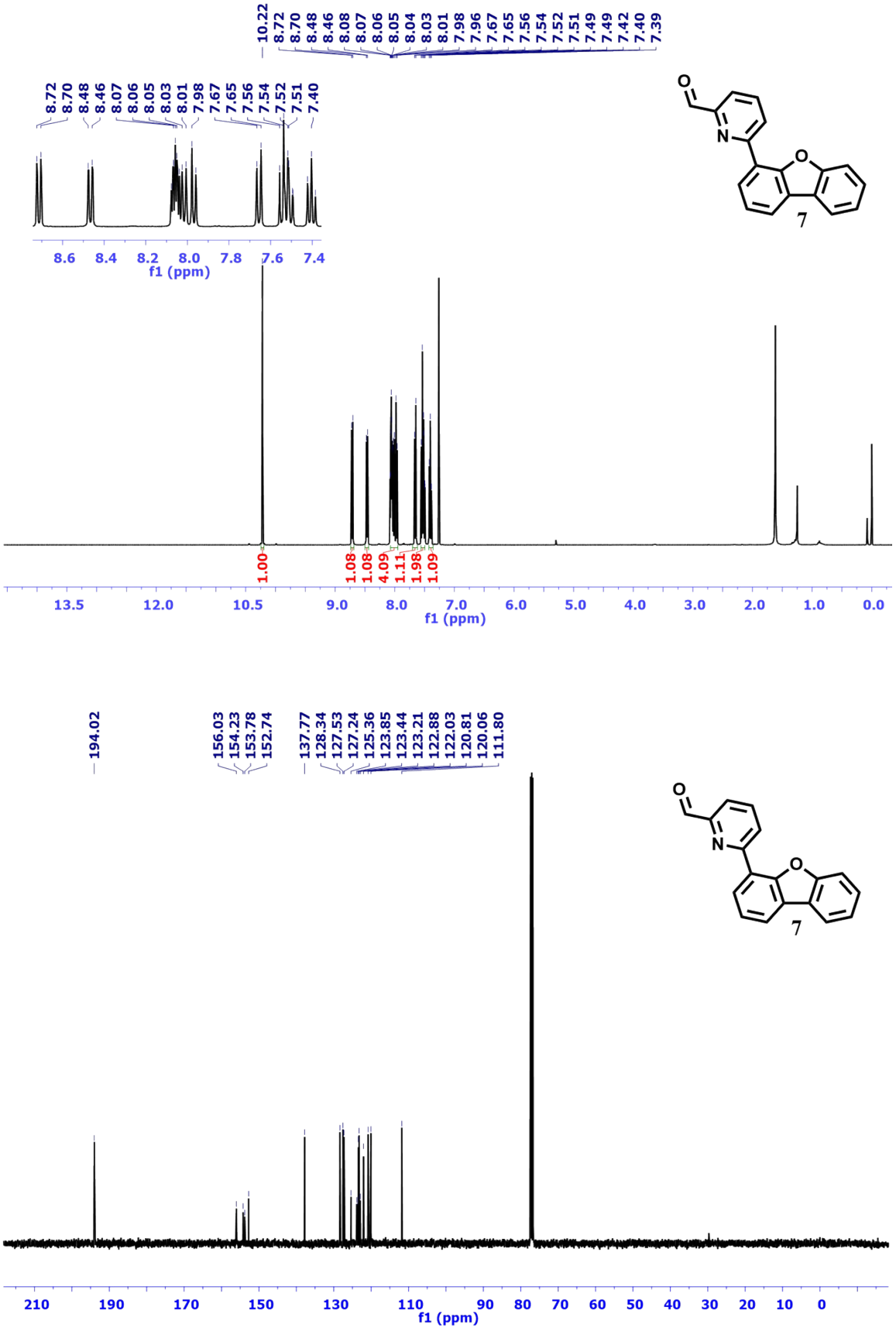

Figure S7: ^{1}H and ^{13}C NMR spectra of compound **7**

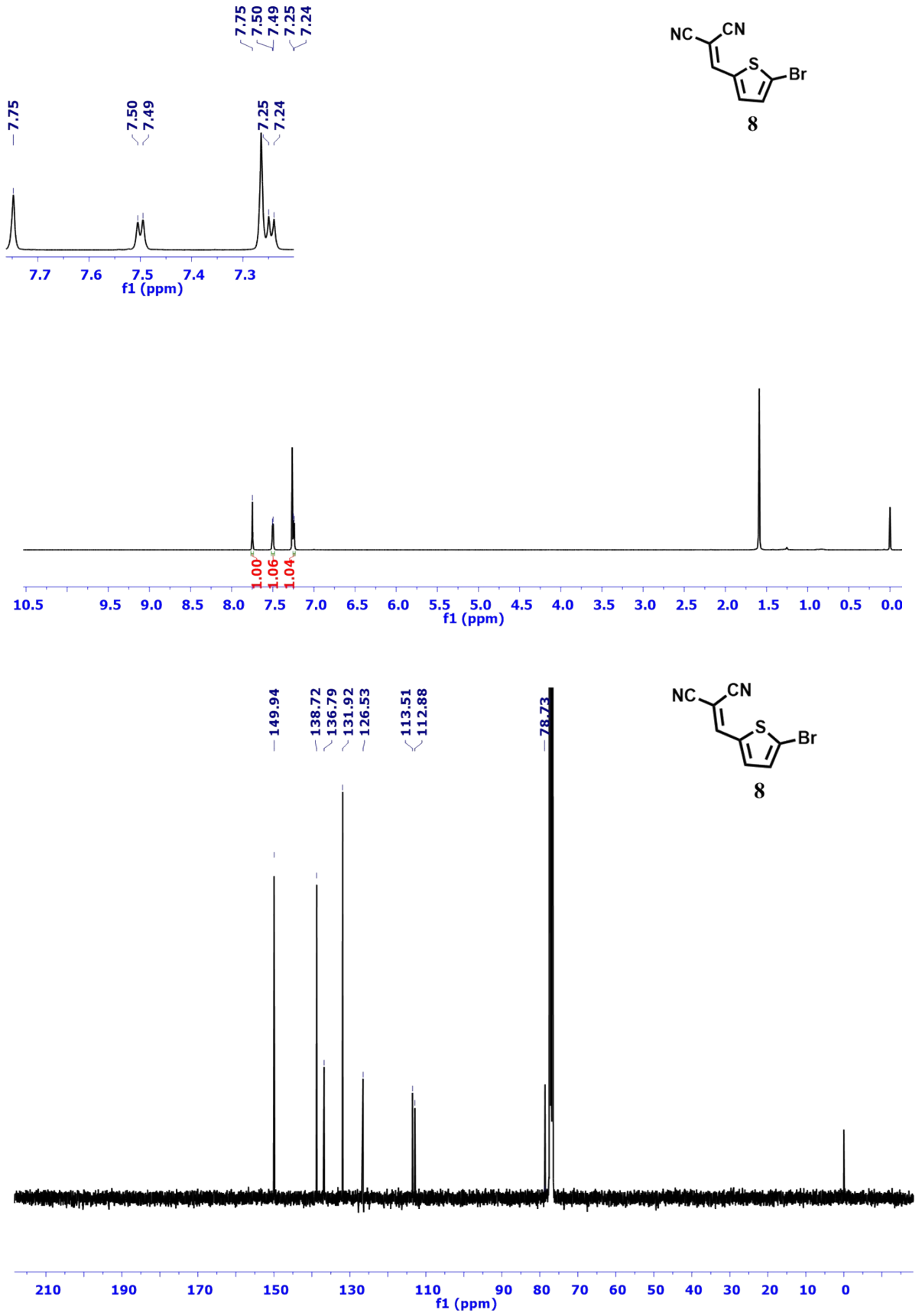

Figure S8: ^{1}H and ^{13}C NMR spectra of compound **8**

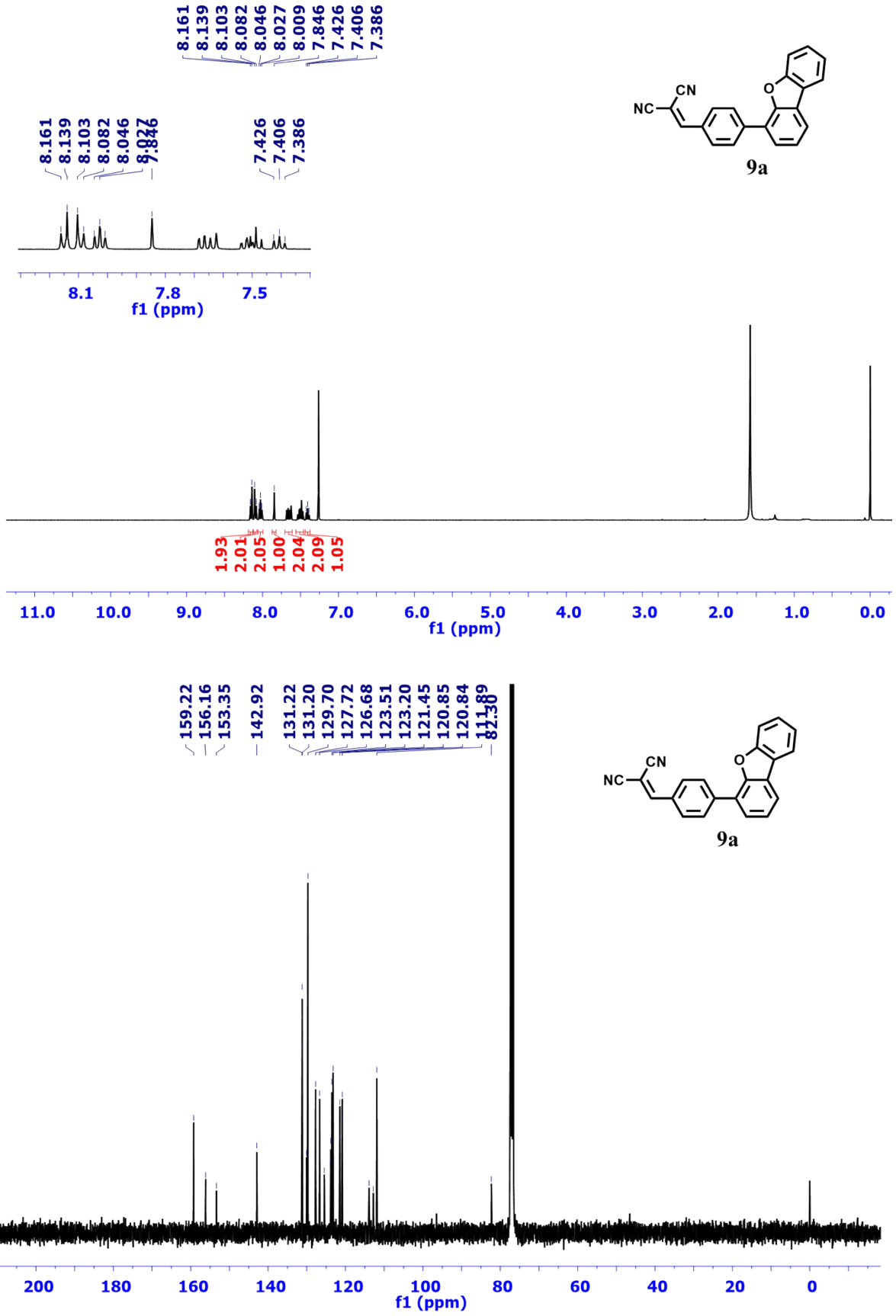

Figure S9: ^{1}H and ^{13}C NMR spectra of compound **9a**

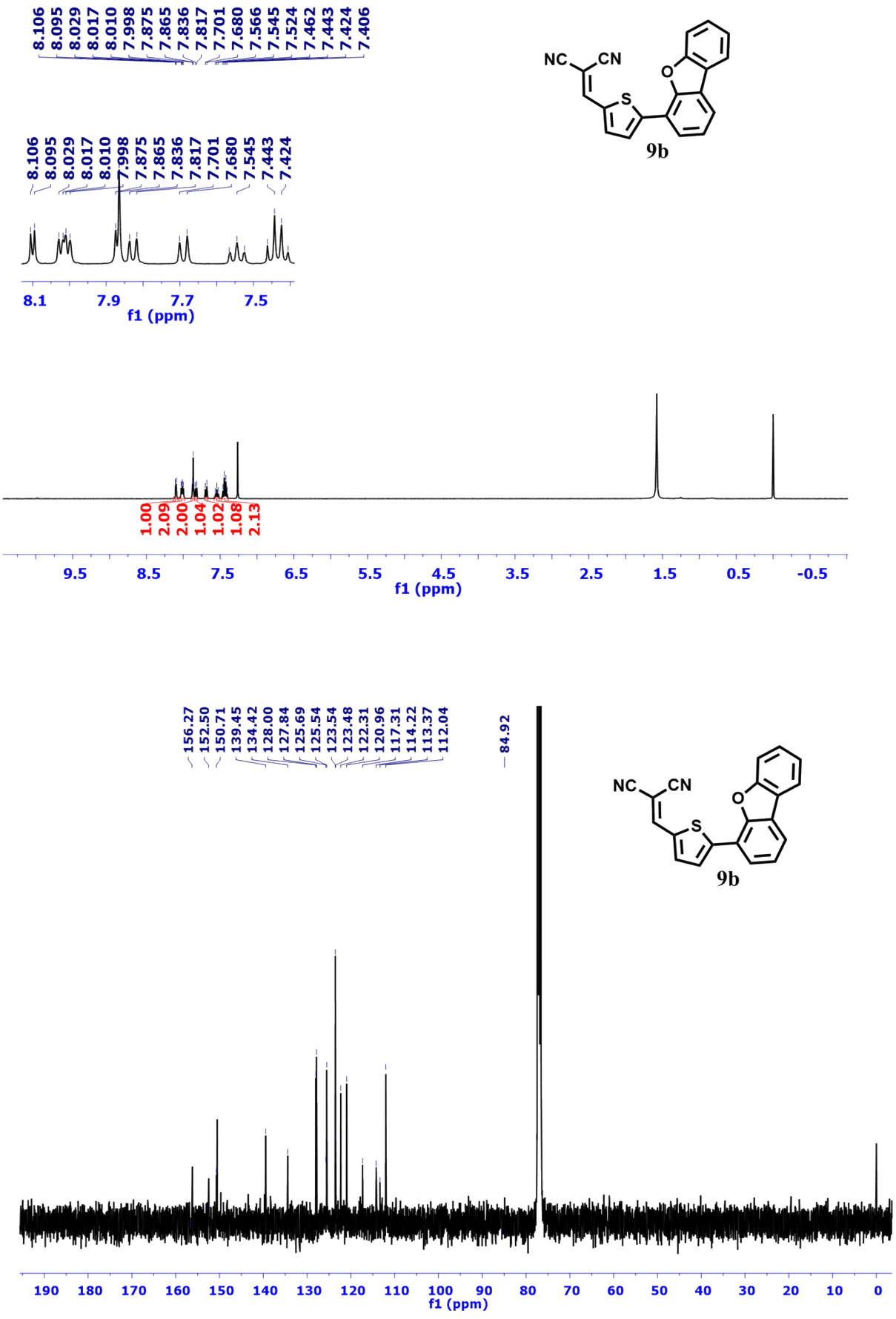

Figure S10: ^{1}H and ^{13}C NMR spectra of compound **9b**

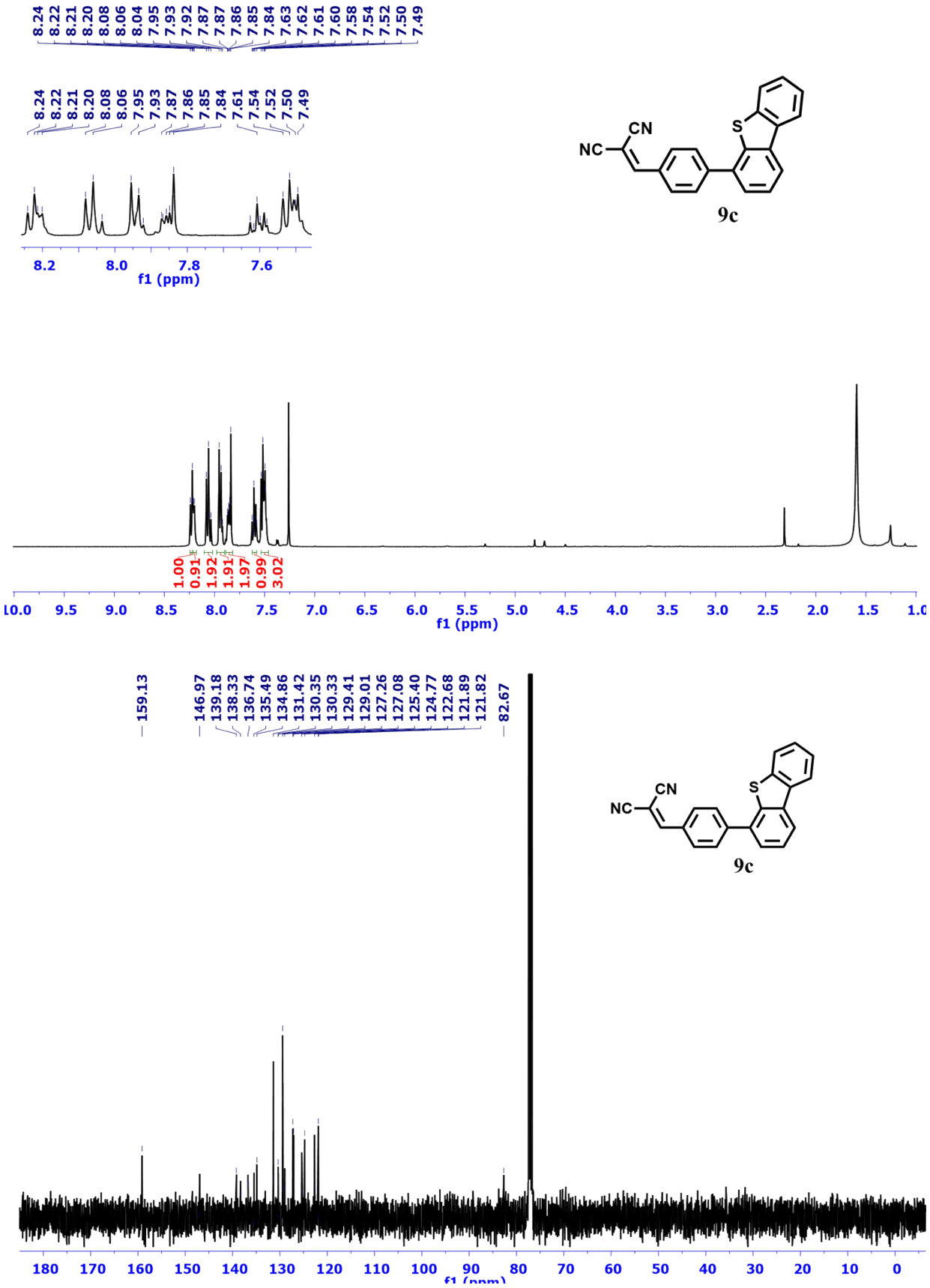

Figure S11: ^{1}H and ^{13}C NMR spectra of compound **9c**

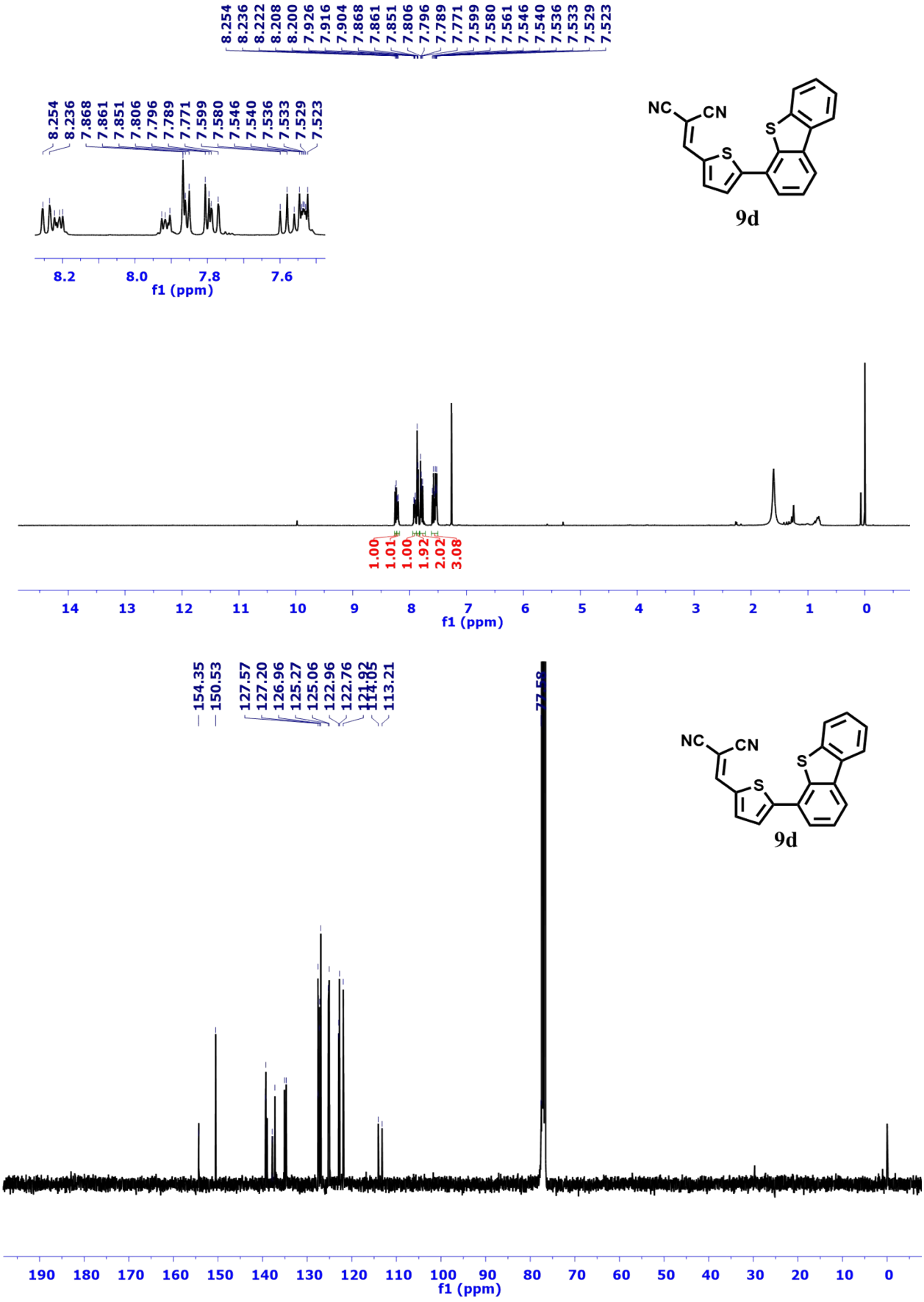

Figure S12: ^{1}H and ^{13}C NMR spectra of compound **9d**

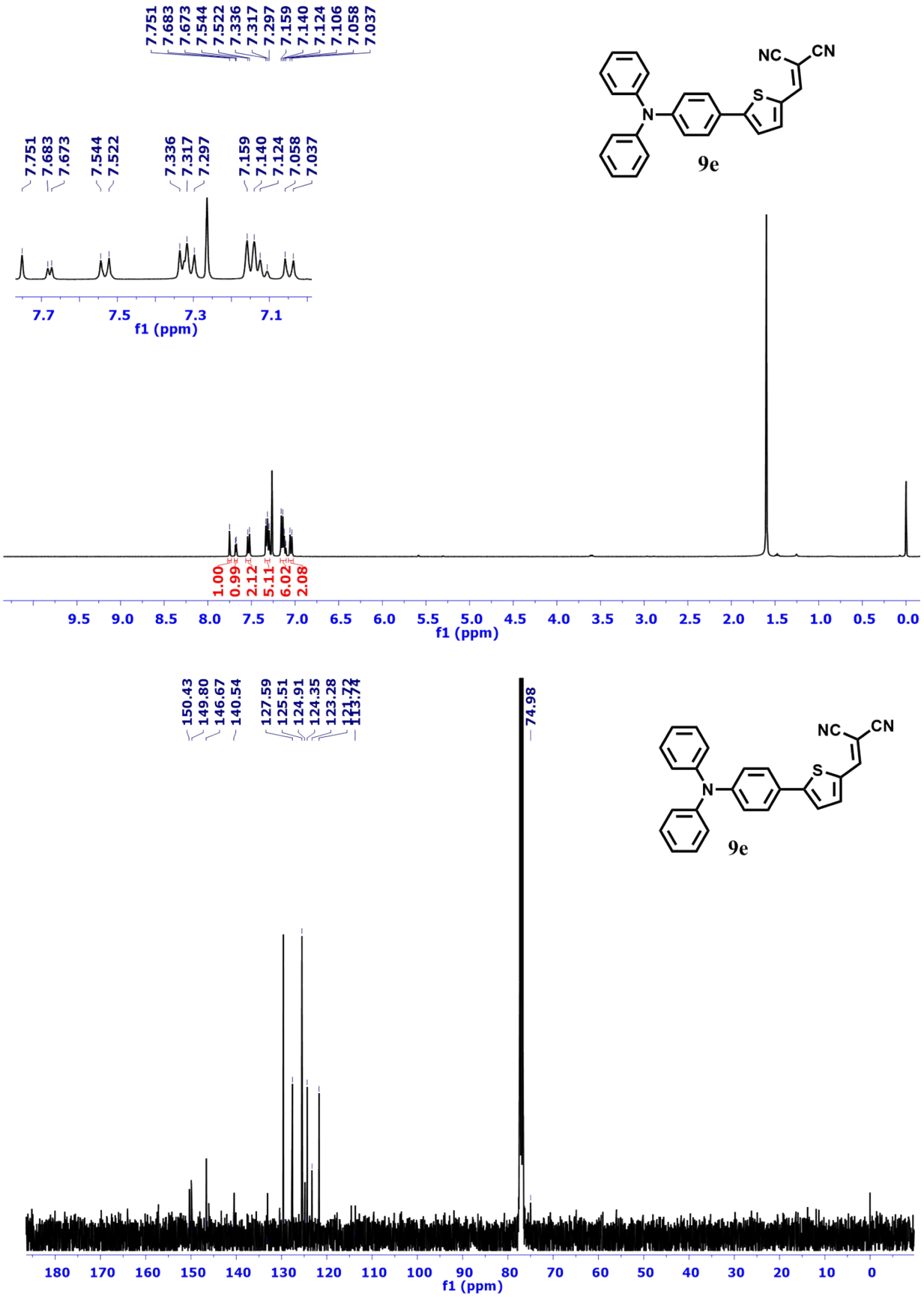

Figure S13: ^{1}H and ^{13}C NMR spectra of compound **9e**

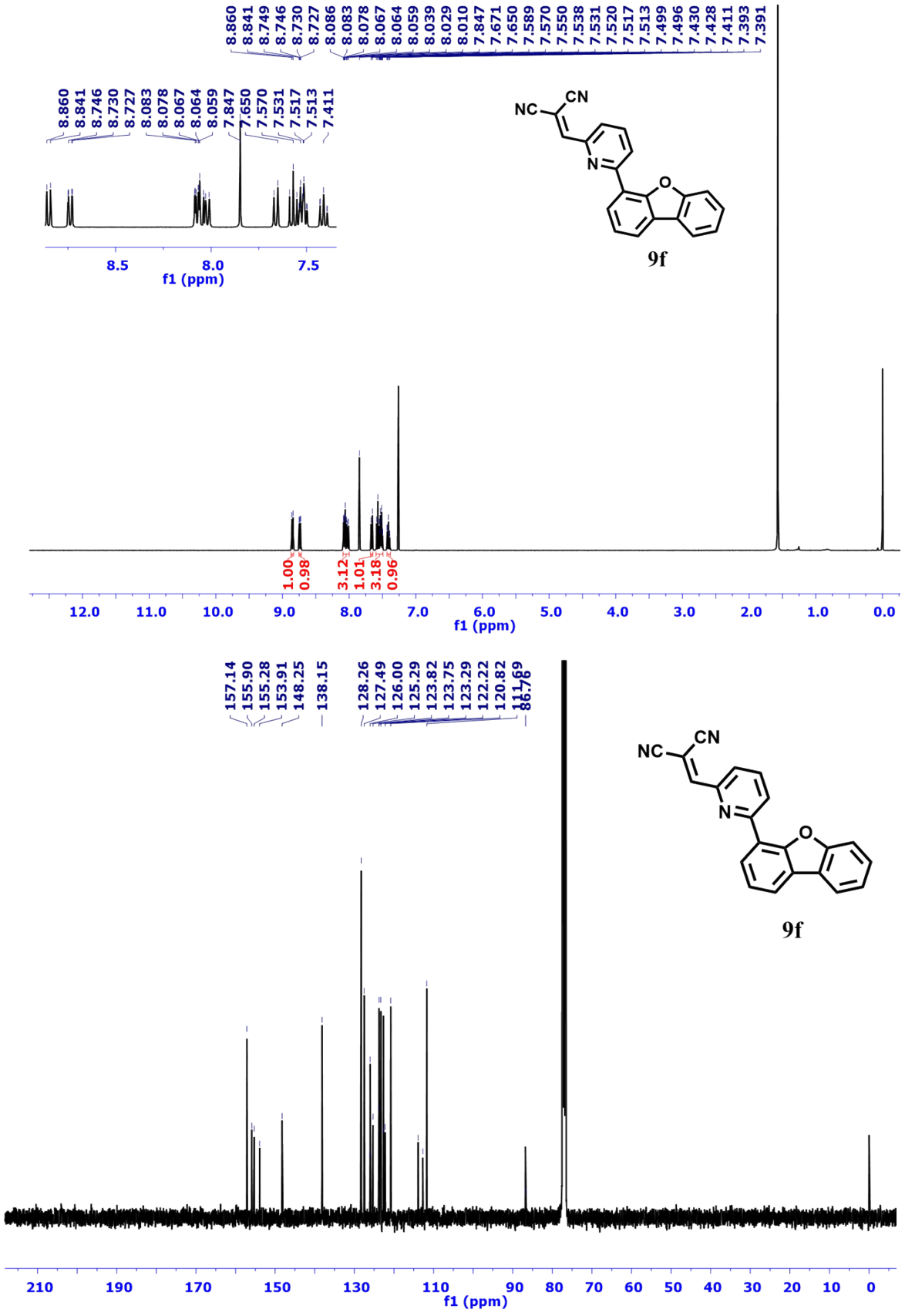

Figure S14: ^{1}H and ^{13}C NMR spectra of compound **9f**

HRMS Spectra of compounds 9a-f

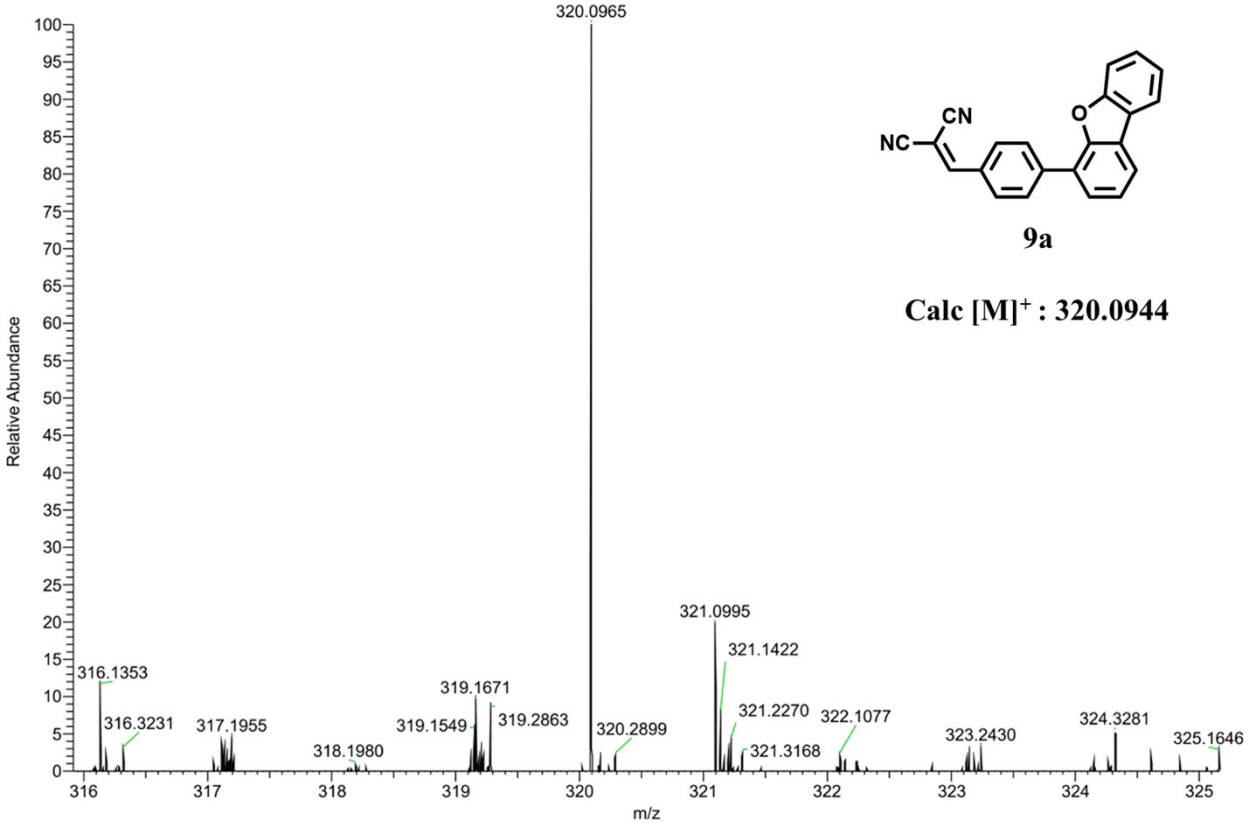

Figure S15: HRMS spectrum of compound **9a**

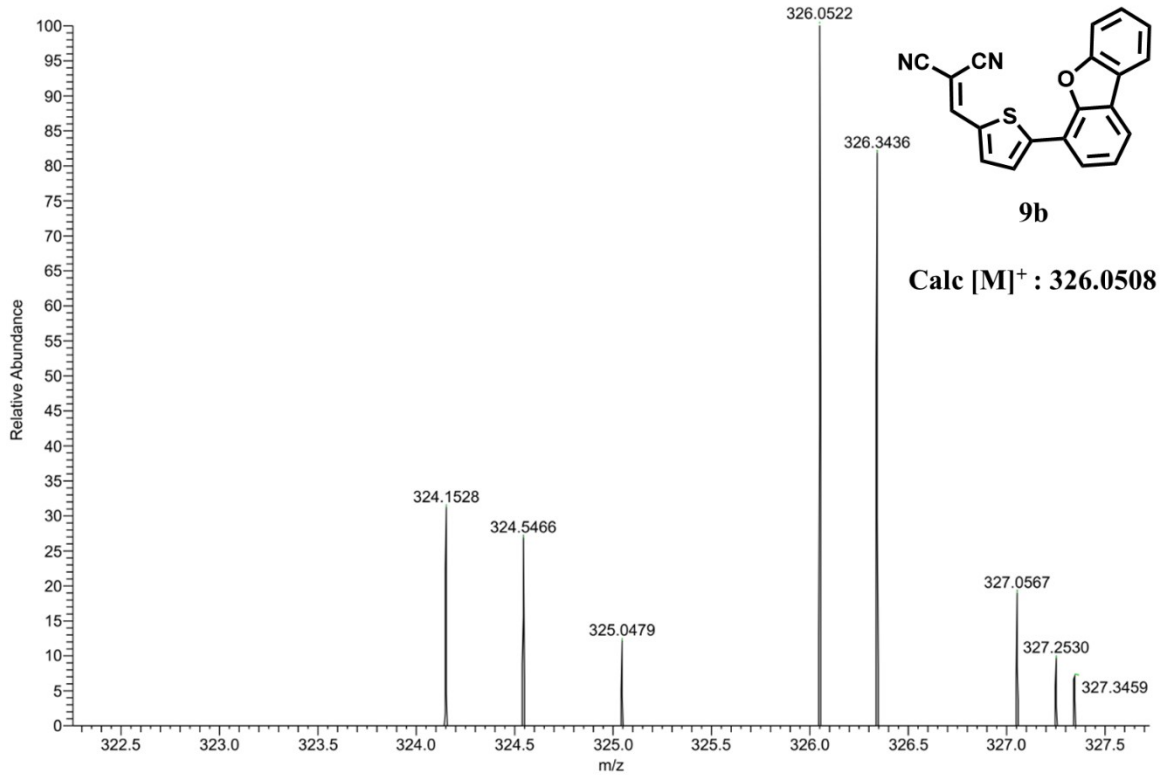

Figure S16: HRMS spectrum of compound **9b**

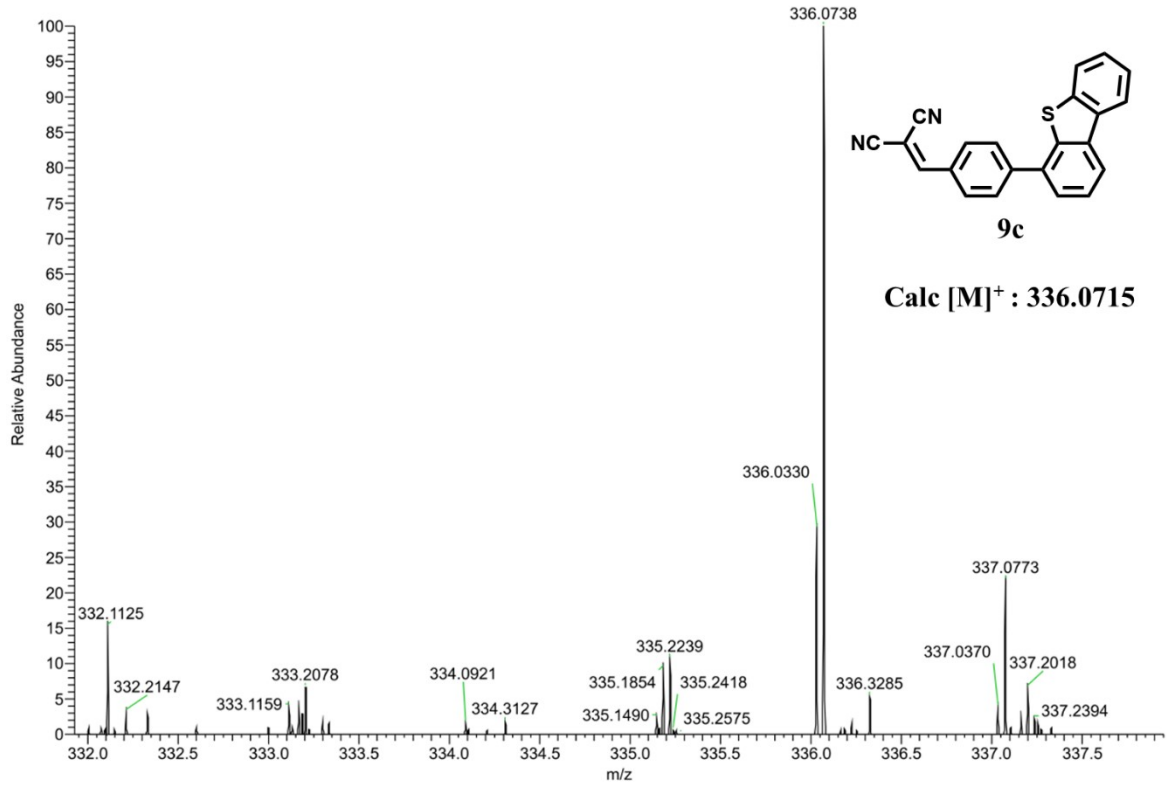

Figure S17: HRMS spectrum of compound **9c**

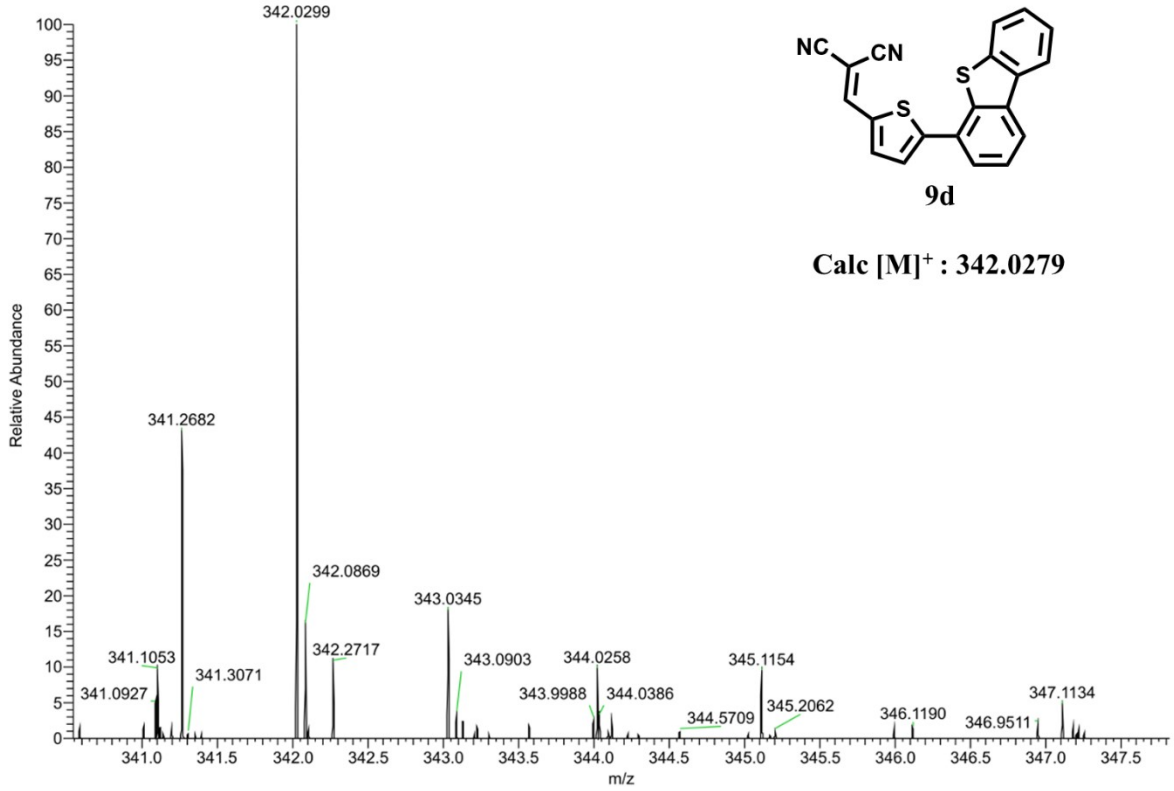

Figure S18: HRMS spectrum of compound **9d**

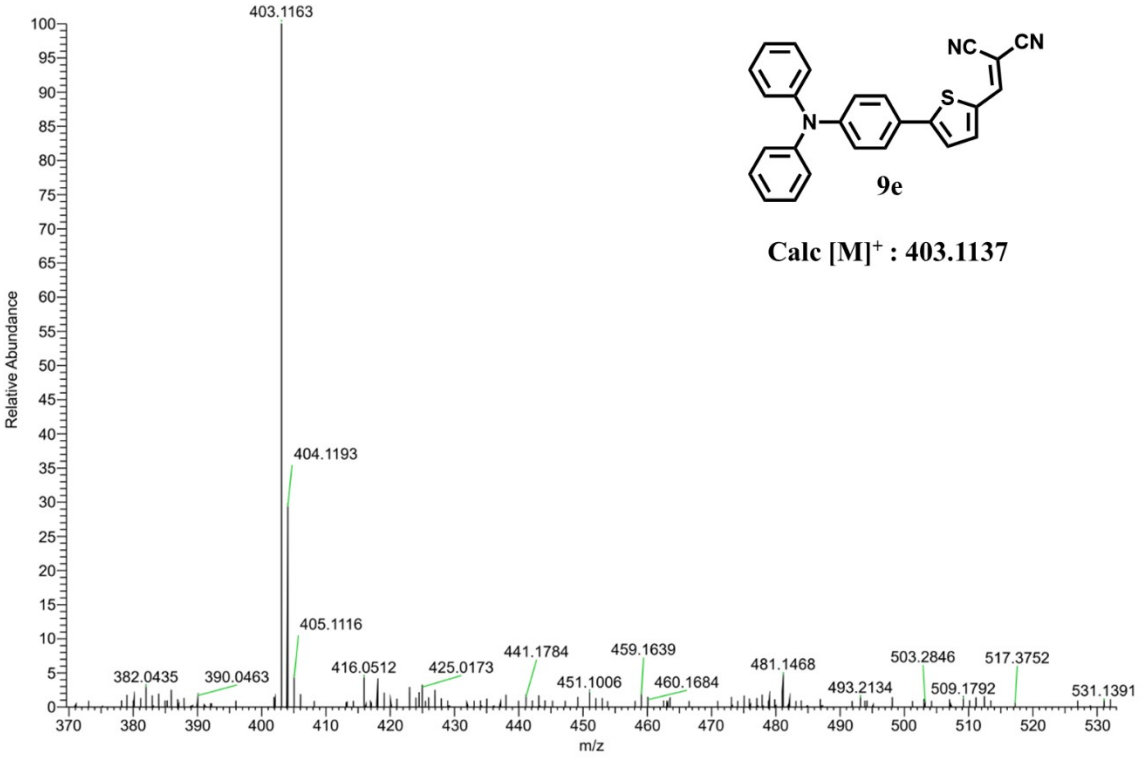

Figure S19: HRMS spectrum of compound **9e**

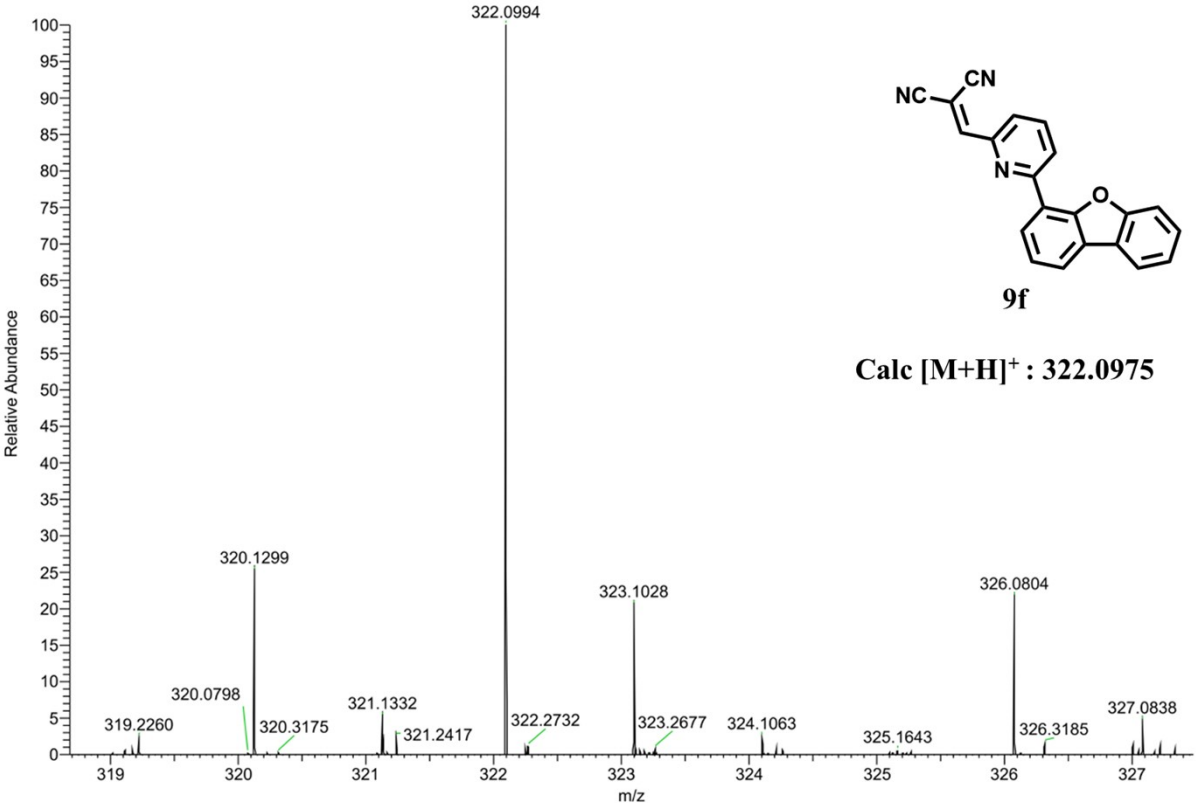

Figure S20: HRMS spectrum of compound **9f**

FT-IR spectra of compounds 9a-f

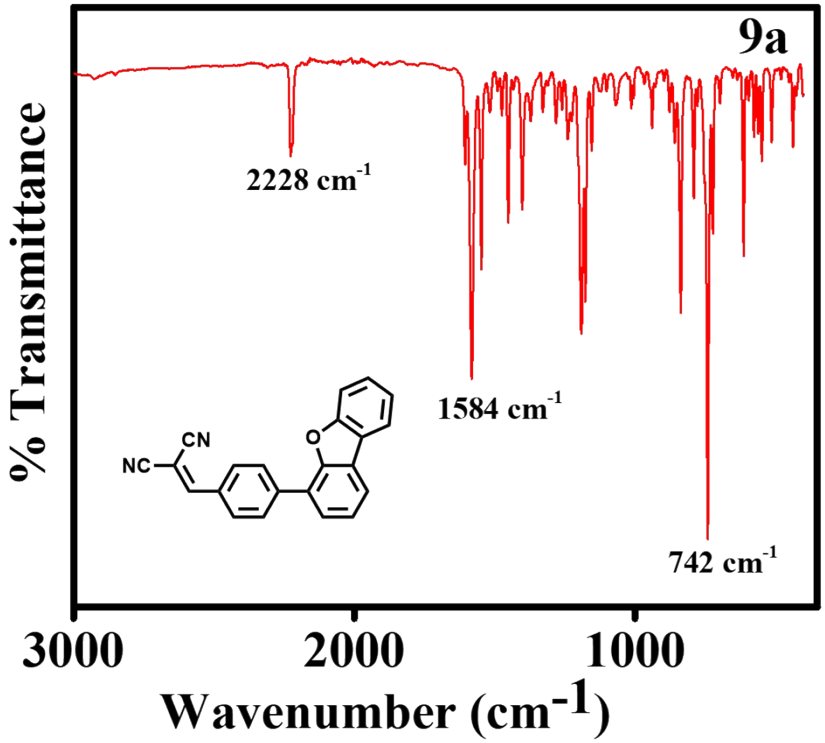

Figure S21: FT-IR spectrum of compound **9a**

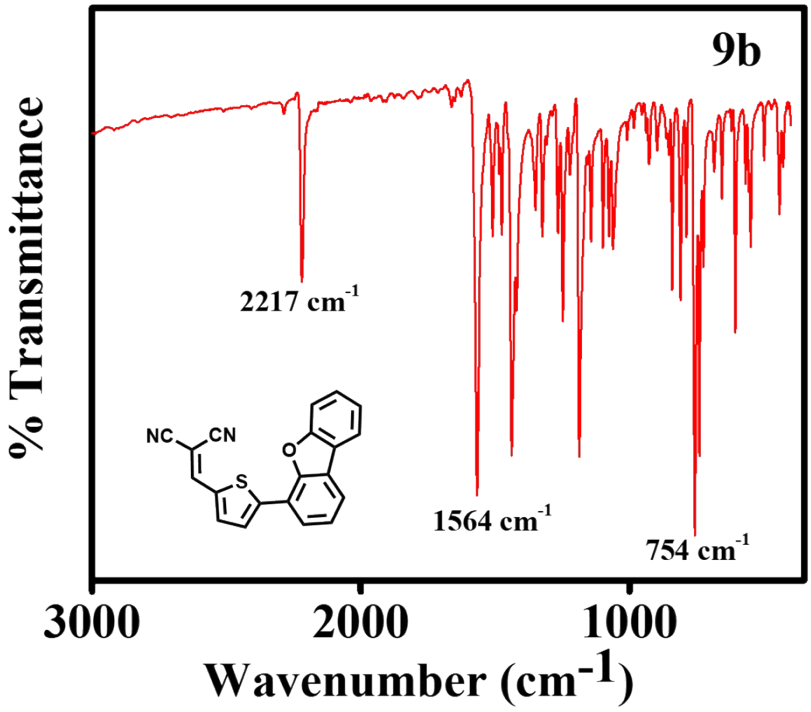

Figure S22: FT-IR spectrum of compound **9b**

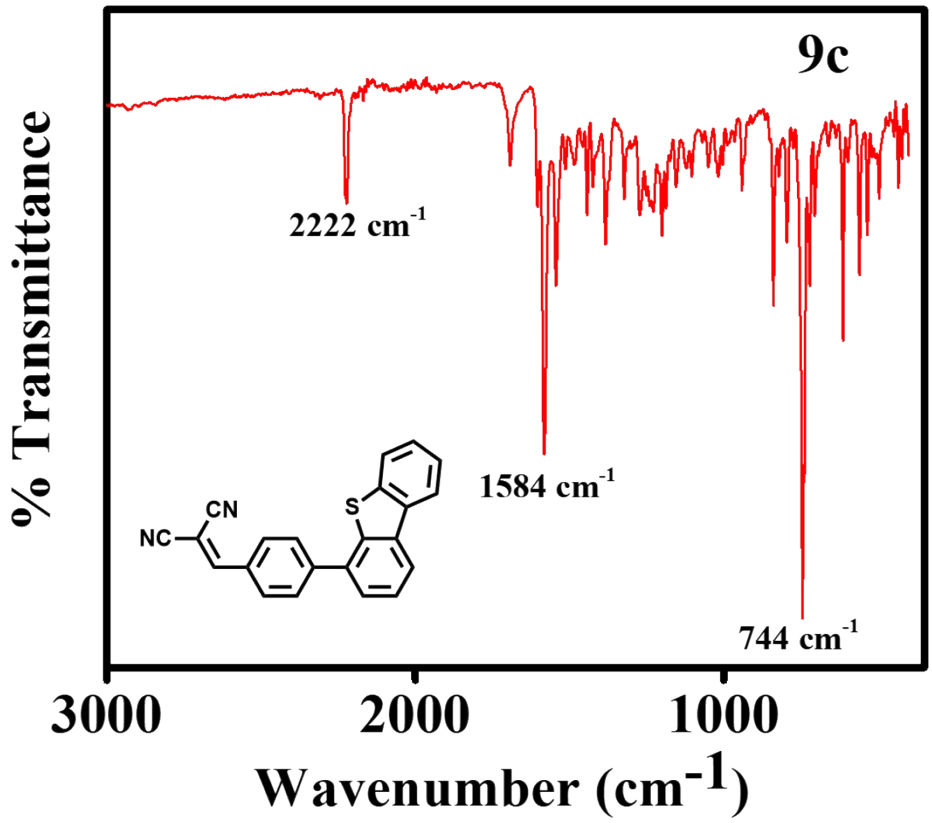

Figure S23: FT-IR spectrum of compound **9c**

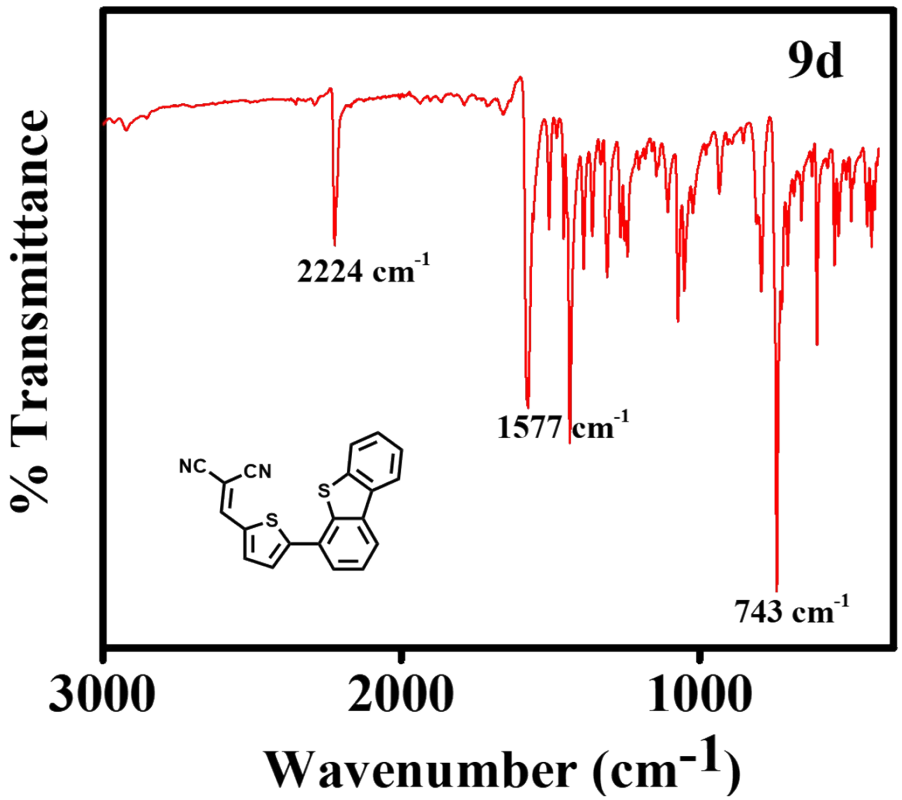

Figure S24: FT-IR spectrum of compound **9d**

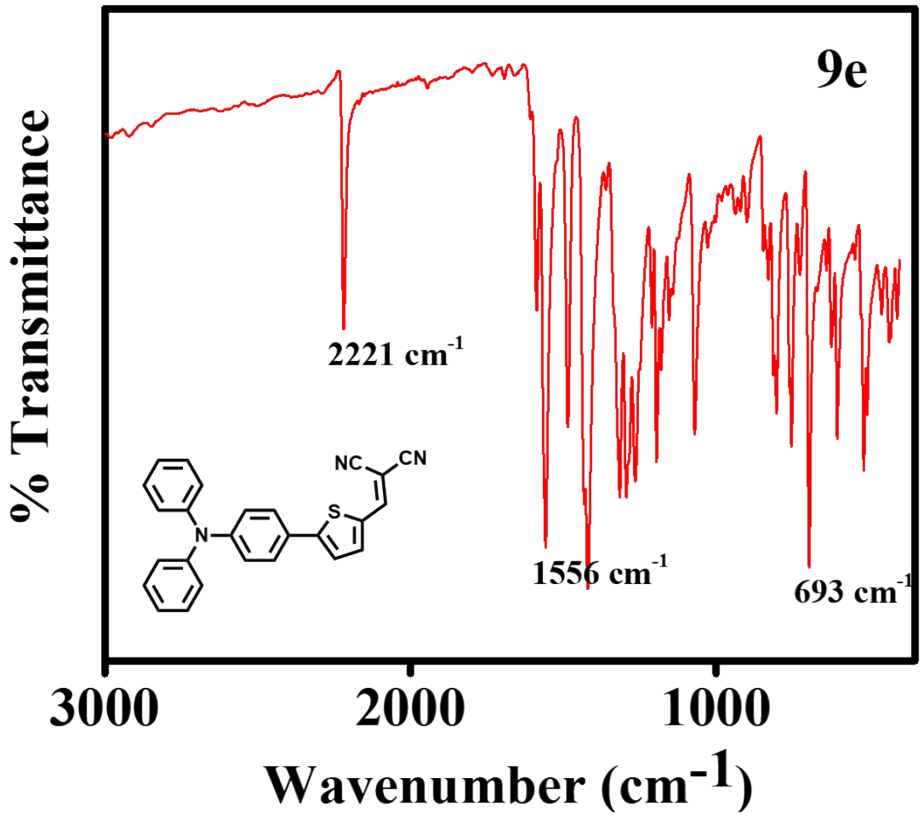

Figure S25: FT-IR spectrum of compound **9e**

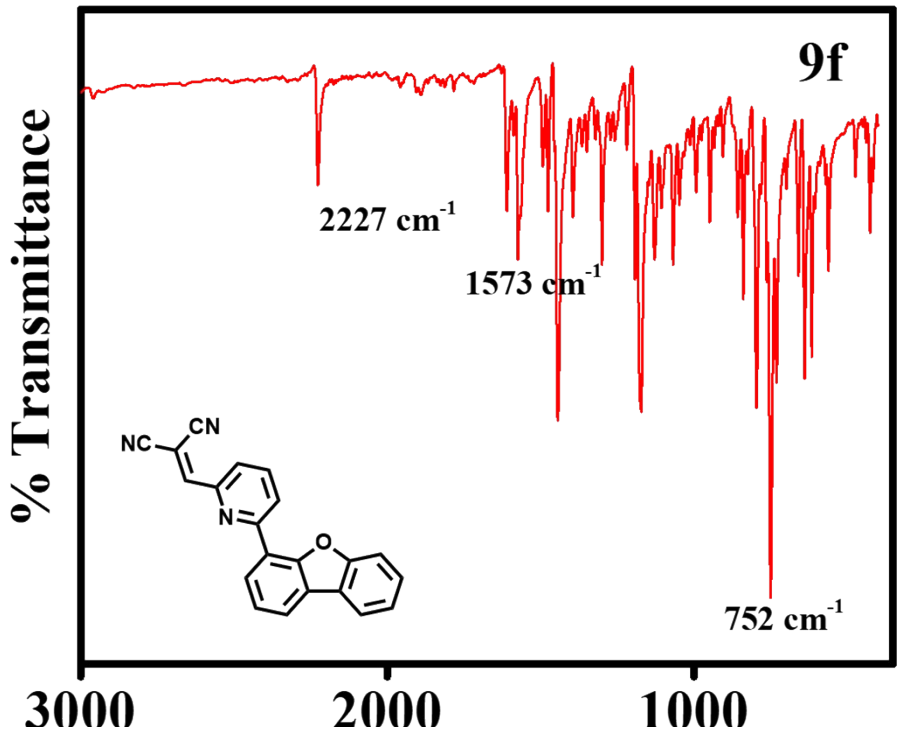

Figure S26: FT-IR spectrum of compound **9f**

4. Single crystal analysis data of compound 9b

CCDC	**2352418**	
Empirical formula	$C_{20}H_{10}N_2OS$	
Formula weight	326.36	
Temperature	100 K	
Wavelength	1.54184 Å	
Crystal system	Monoclinic	
Space group	$P2_1/n$	
Unit cell dimensions	a = 8.54080(4) Å	α= 90 °.
	b = 16.20195 (11) Å	β= 92.7345(5)°.
	c = 22.03161(13) Å	γ = 90°.
Volume	3045.21(3) $Å^3$	
Z	8	
Density (calculated)	1.424 Mg/m^3	
Absorption coefficient	0.634 mm^{-1}	
F(000)	1344.0	
Crystal size	0.87×0.18×0.11 mm^3	
Theta range for data collection	3.387 to 74.476 °.	
Index ranges	-8<=h<=10, -18<=k<=20, -27<=l<=28	
Reflections collected	32619	
Independent reflections	6222 [R(int) = 0.0292]	
Completeness to theta = 74.476 °	72 %	
Absorption correction	0.721 mm^{-1}	
Max. and min. transmission	0.683 and 0.804	
Refinement method	Full-matrix least-squares on F^2	
Goodness-of-fit on F^2	1.058	
Final R indices [I >2sigma(I)]	R1 = 0.0304 , wR_2 = 0.0847	
R indices (all data)	R1 = 0.0319, wR_2 = 0.0860	
Extinction coefficient	n/a	

Single crystal analysis data of compound 9f

CCDC	**2352451**	
Empirical formula	$C_{21}H_{11}N_3O$	
Formula weight	321.33	
Temperature	100 K	
Wavelength	1.54184 Å	
Crystal system	Monoclinic	
Space group	$P2_1/c$	
Unit cell dimensions	a = 7.42920(10) Å	α= 90 °.
	b = 15.49490(10) Å	β= 101.3150(10) °.
	c = 13.35450(10) Å	γ = 90°.
Volume	1507.42(3) $Å^3$	
Z	4	
Density (calculated)	1.416 Mg/m^3	
Absorption coefficient	0.721 mm^{-1}	
F(000)	664.0	
Crystal size	0.69 × 0.26 × 0.07 mm^3	
Theta range for data collection	4.421 to 74.461 °.	
Index ranges	-8<=h<=9, -18 <=k<= 19, -16<=l<= 17	
Reflections collected	15770	
Independent reflections	3090 [R(int) = 0.0216]	
Completeness to theta = 74.476 °	73 %	
Absorption correction	0.721 mm^{-1}	
Max. and min. transmission	0.796 and 0.953	
Refinement method	Full-matrix least-squares on F^2	
Goodness-of-fit on F^2	1.029	
Final R indices [I >2sigma(I)]	R1 = 0.0325 , wR_2 = 0.0852	
R indices (all data)	R1 = 0.0342, wR_2 = 0.0865	
Extinction coefficient	n/a	

5. Thermogravimetric analysis

Table S1. Thermal properties of compounds **9a-f**

Compounds 9	Td(°C)*
a	296.54
b	320.05
c	310.14
d	320.18
e	325.60
f	293.06

*Td is a decomposition temperature

6. Electrochemical studies of the compounds 9a-f

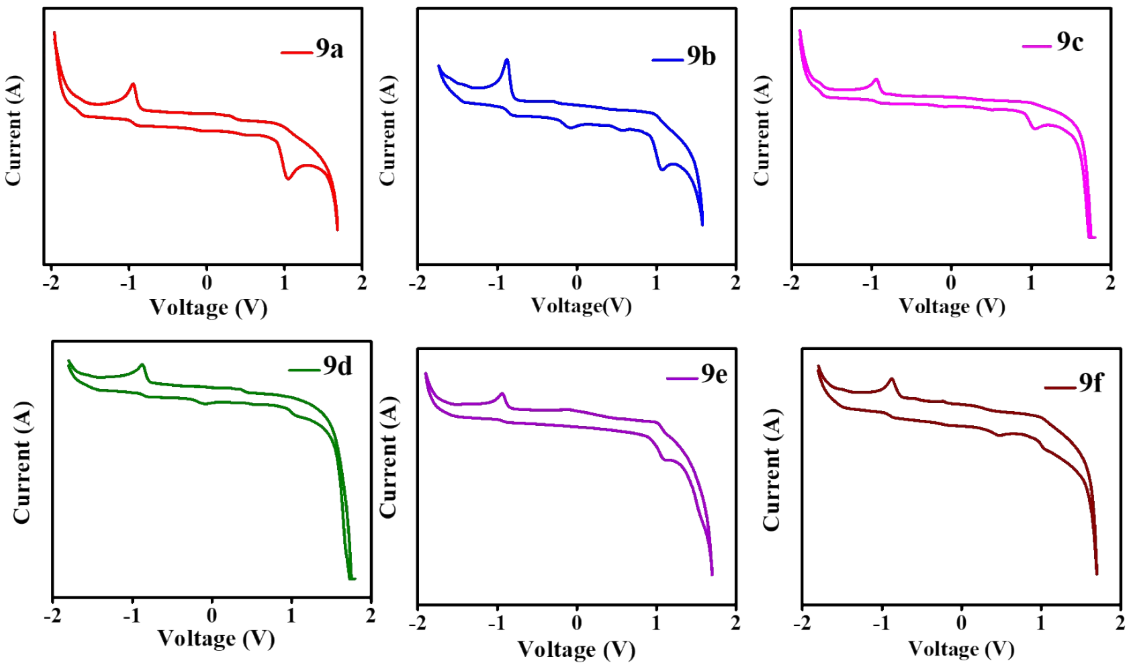

Figure S27. Cyclic voltammogram of compounds **9a-f**

7. Thin-film morphological studies of the compounds 9a-c

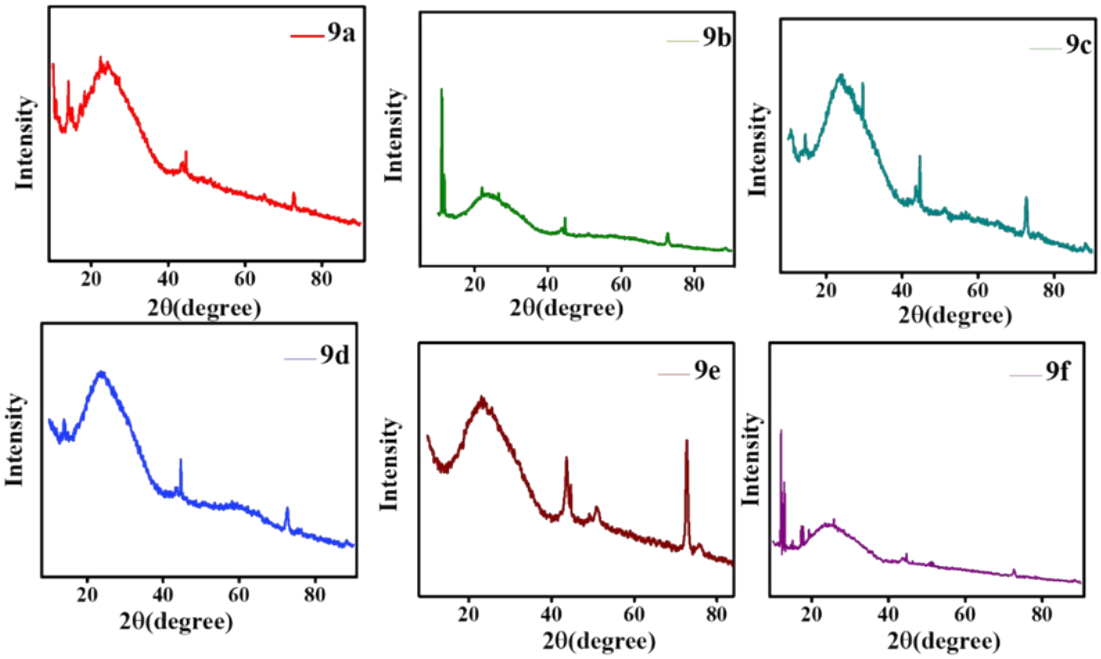

Figure S28. Thin-film GIXRD of compounds **9a-f**

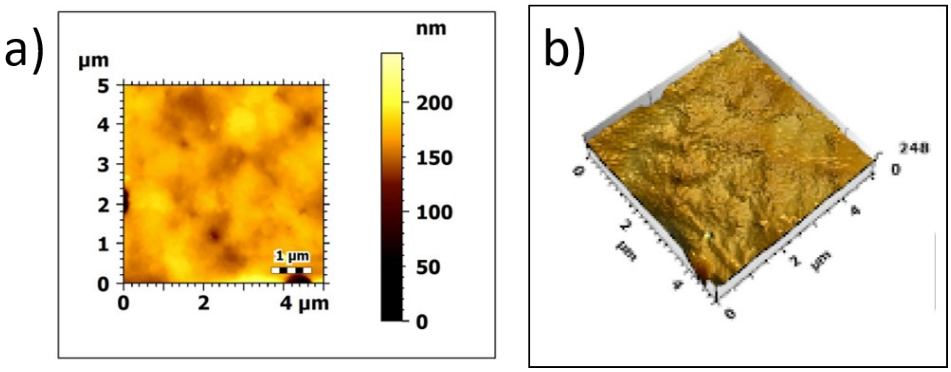

Figure S29: (a) Atomic Force Microscope image of the thin film of compound **9a (b)** AFM three-dimensional image of compound **9a**

8. Stability tests of the device

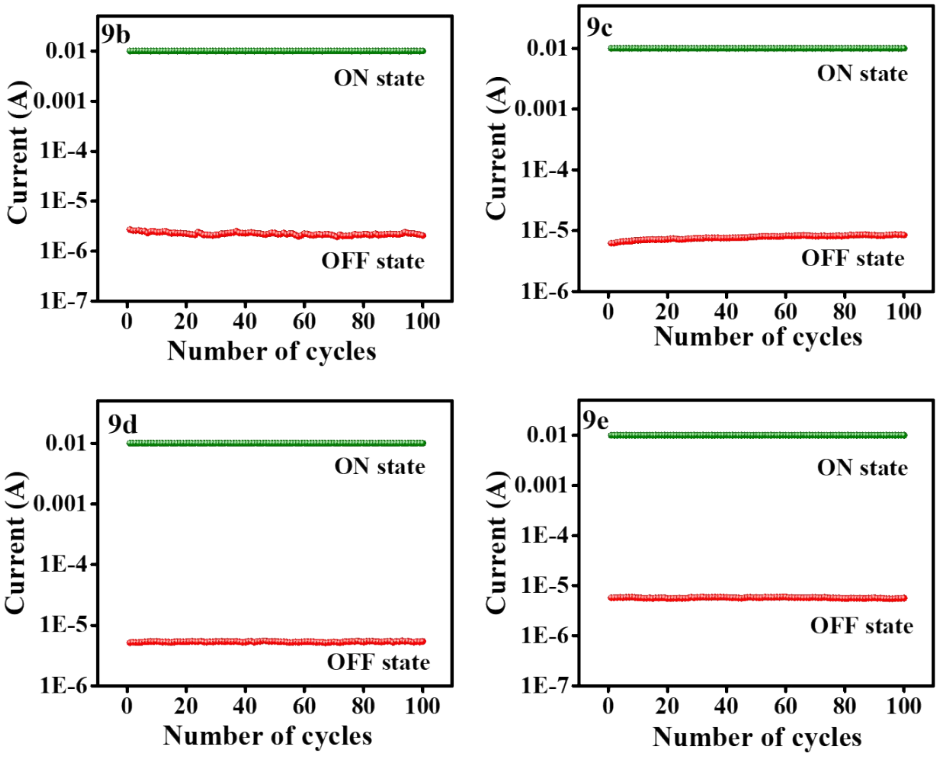

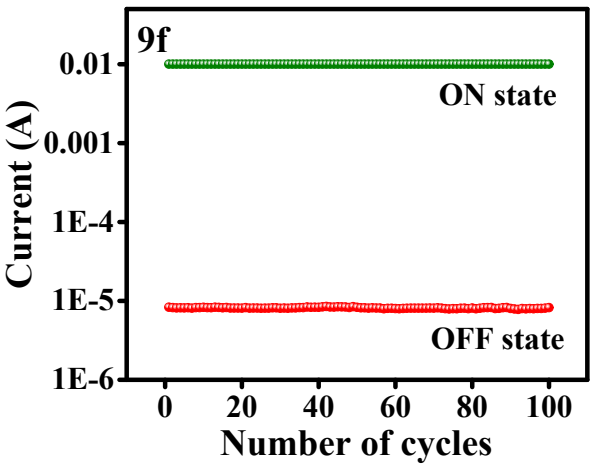

Figure S30: Endurance cycle for devices ITO/9b-f/Ag

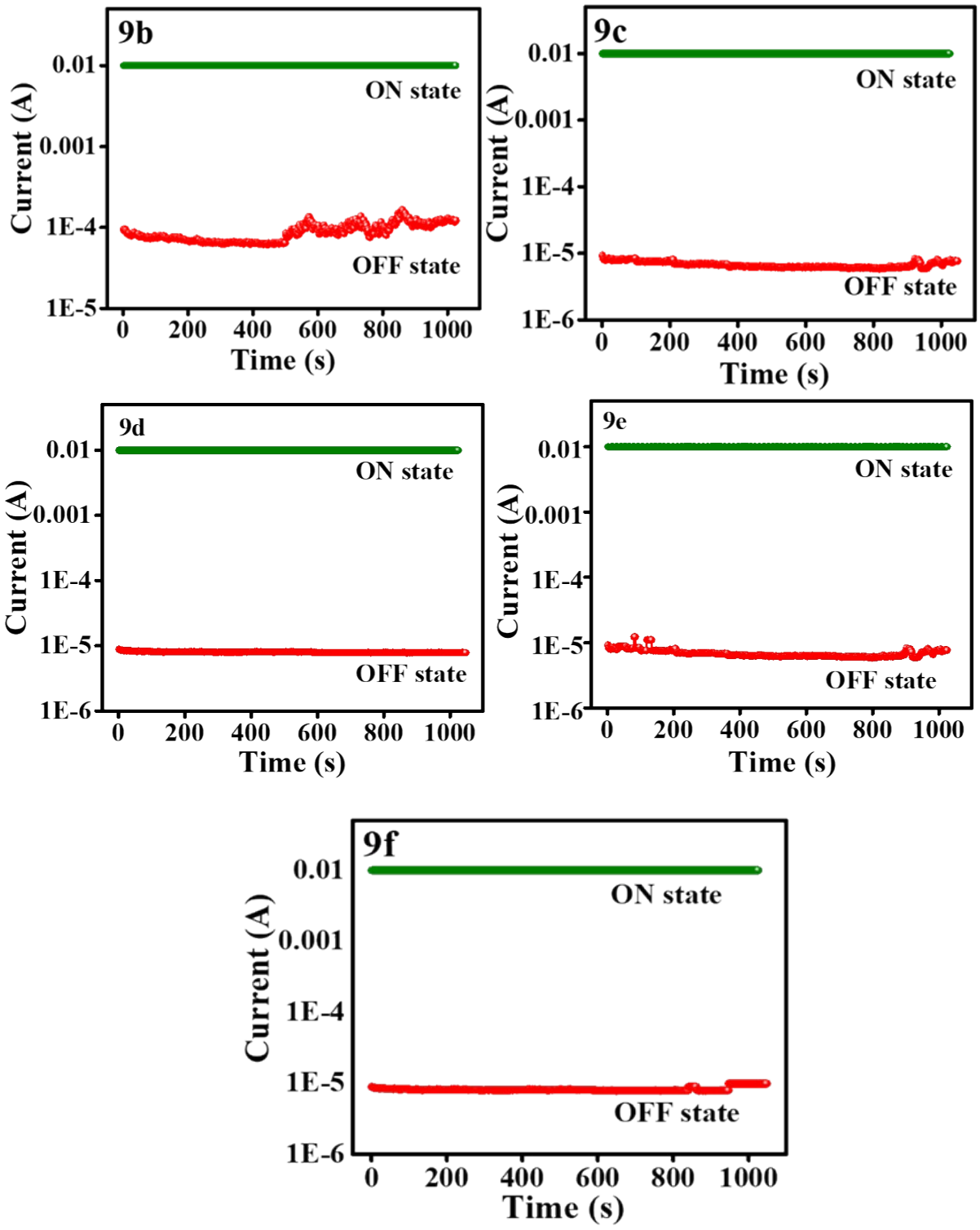

Figure S31: Retention time of the devices ITO/9b-f/Ag

9. Yield of the devices.

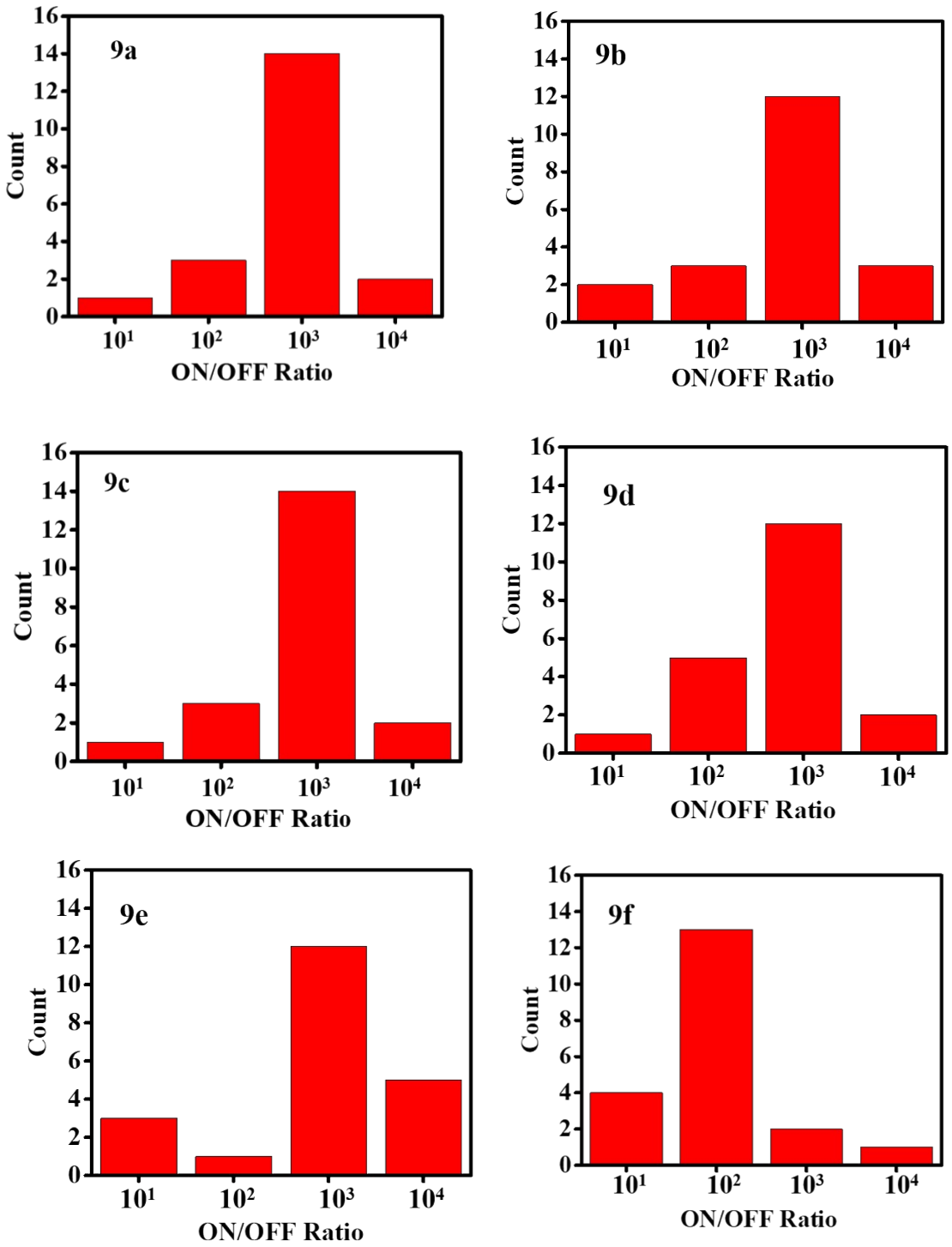

Figure S32: Yield of the devices ITO/9b-f/Ag

10. Computational studies

Experimentally determined spectral values were compared with the computationally derived excited states of the molecules (**Table S2**). Time Dependent-Self Consistent Field (TD-SCF) theoretical calculations provided significant insights into the spectral characteristics. The absorption and emission bands observed experimentally match the theoretical predictions. Furthermore, the calculations showed a remarkable capability to predict the emission spectral values accurately. Only theoretical predictions with favourable frequency factors and close agreement with experimental observations are selected from the pool of proposed values. Notably, the prediction of intersystem crossing in nearly all the systems aligns with the observed emission spectra. The density of states (DOS) can be defined as the number of distinct electronic states permissible at a specific energy level per unit volume per unit of energy. This function is crucial in determining the bulk properties of conductive solids, including specific heat, paramagnetic susceptibility, and various transport phenomena.

Table S2: The predicted absorption and emission behaviour of the compounds **9a-f**

Compounds 9	**Absorption wavelength (nm)**	**Electronic transition**	**Emission wavelength (nm)**	**Electronic transition**	**Dipole moment**
a	389	S_{-1} -S_{1}	405	S_0-S_1	8.15
b	347	S_{-2}-S_{-1}	412	S_0-S_1	8.63
c	399	S_{-1}-S_1	496	S_0-S_1	8.26
d	454	S_{-1}-S_1	400	S_0-S_1	8.60
e	462	S_{-1}-S_1	521	S_0-S_1	10.73
f	337	S_{-4}-S_1	428	S_0-S_1	7.85

Following geometry optimization, the resulting optimal geometry was employed as the input for Density of States (DOS) calculations utilizing the Vienna Ab initio Simulation Package (VASP) software (MedeA reference) (**Figure S33**). Structures incorporating Wentzell correction parameters, such as GGA-PBE (basis set), were evaluated, and the DOS was subsequently obtained. The density of states (DOS) graph depicts the number of available energy states, which can be interpreted as the optimal space for particle movement within the material. Table S2 details the DOS gap and Fermi energy levels for each compound. Compounds **9a-c** and **9f** exhibit a higher number of states with respective DOS gaps of 2.96 and 4.01 eV. These narrow band gaps theoretically indicate significant electronic conjugation

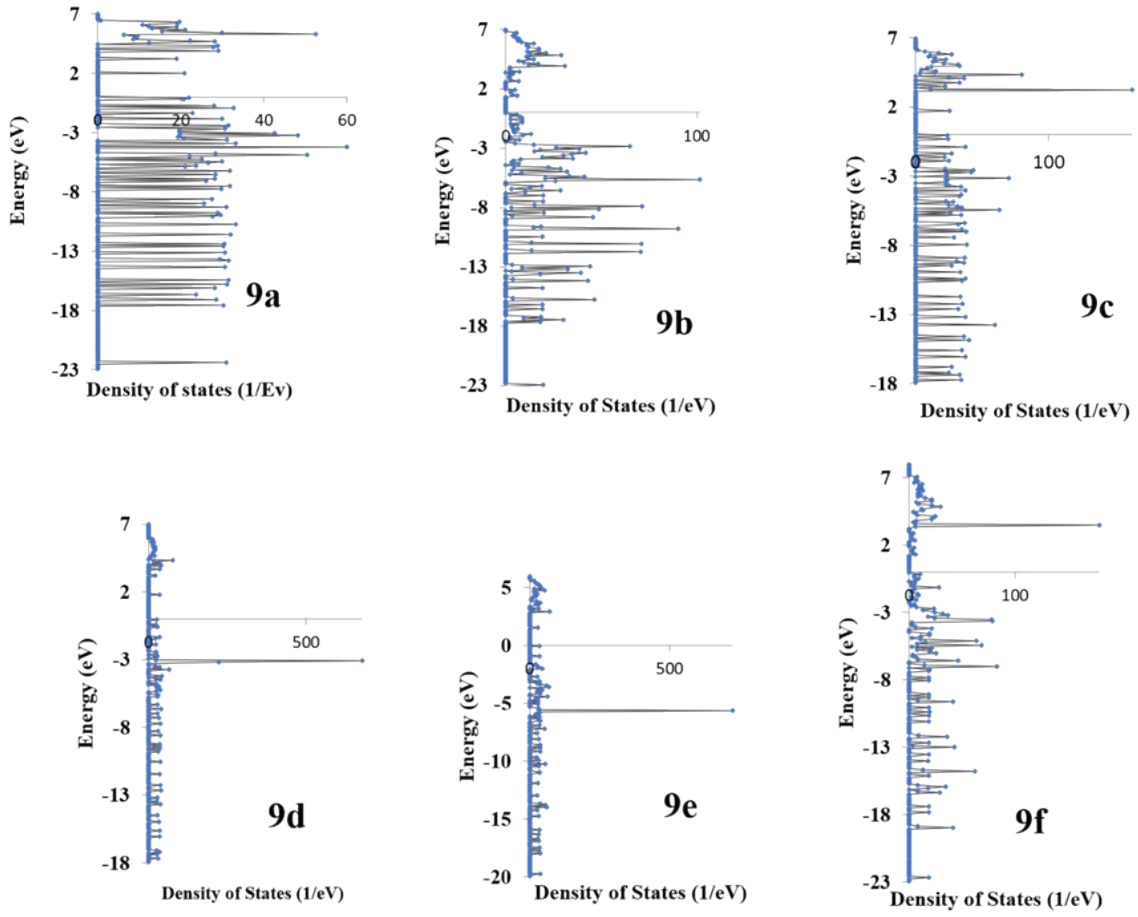

within these compounds.

Figure S33: Density of States graphs for the compounds 9a-f

Compounds 9	Molecular Formula	Free Energy (eV)	Density (Mg/m^3)	DOS gap (eV)	Band gap (eV)	E Fermi (eV)
a	$C_{22}H_{12}N_2O$	-263.30	0.356	2.959	2.056	-4.381
b	$C_{20}H_{10}N_2OS$	-241.74	0.635	2.956	1.965	-2.834
c	$C_{22}H_{12}N_2S$	-260.95	0.343	2.961	1.786	-4.176
d	$C_{20}H_{10}N_2S_2$	-239.35	0.398	2.963	1.849	-3.975
e	$C_{26}H_{17}N_3S$	-322.92	0.331	2.134	1.501	-3.641
f	$C_{22}H_{12}N_3O$	-258.53	0.615	4.014	1.877	-3.109

Table S3 : DOS gap and E-Fermi energy of the compounds 9a-f

In accordance with single-crystal X-ray diffraction data, which provides a static picture of a molecule, MedeA modeling with solvent correction can simulate the behaviour of molecules in solution, mimicking real-world conditions of normal temperature and pressure. **Figure S34** depicts the molecular packing of compounds **9a-f**, highlighting their packing efficiency. The data are summarized in **Table S4**. Additionally, computational calculations estimate the hopping distances between molecules, which can inform potential charge transport mechanisms. Compounds **9c** and **9e** exhibit shorter hopping distances of 2.672 and 2.679 Å, respectively, due to their favourable molecular arrangement.

Table S4: Crystal parameters of compounds **9a-f**

Compounds 9	Cell Parameters	Type of the Cell	Preferences	Symmetry	Hopping Distances, A
a	18.5/11.2/7.14 90/90/90	simple orthorhombic	3 2 3	P21-C	3.545 4.151 4.380
b	16.9/12.6/6.00 90/90/90	simple orthorhombic	3 1 4	P21-C	3.479 4.008 4.312
c	19.4/11.7/7.13	simple	1 3 4	P21-C	2.597

	90/90/90	orthorhombic			2.672 3.493
d	18.2/12.1/6.53 90/90/90	simple orthorhombic	2 2 4	P21-C	2.730 4.238 4.914
e	20.6/12.9/7.58 90/90/90	simple orthorhombic	3 4 1	P21-C	2.679 5.788 6.193
f	18.7/11.5/4.01 90/90/90	simple orthorhombic	3 1 4	P21-C	3.126 4.395 5.150

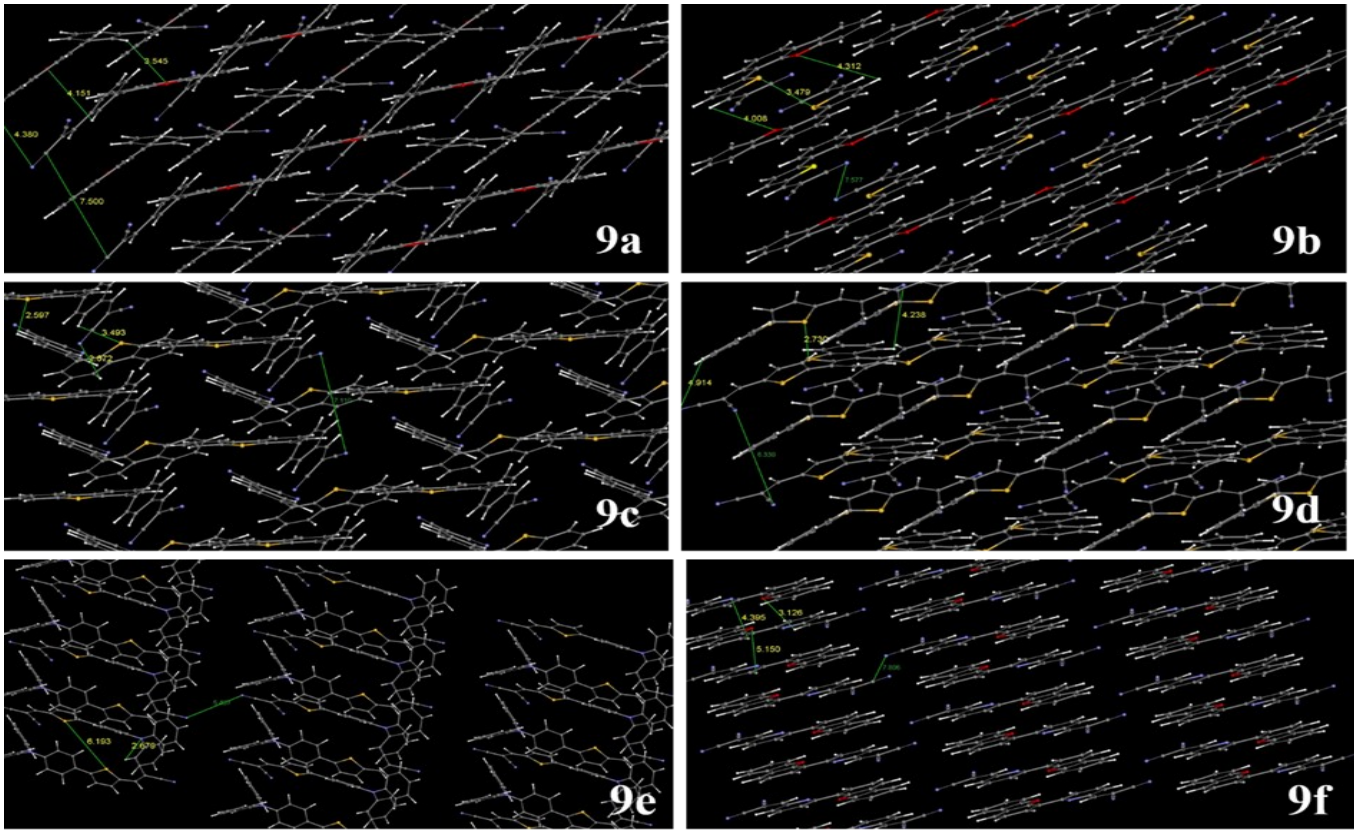

Figure S34: Molecular packing and hopping distances for the compounds **9a-f** through computational methods

11. Fabrication of memory device

The synthesized compounds **(9a-f)** were used as the active layer on an ITO substrate to fabricate the memory devices. The ITO-coated glass plates were meticulously cleaned by sonication in a solution of soap, distilled water, acetone, and ethanol for ten minutes. ITO serves as the bottom electrode in the memory device's construction. The compounds **9a-f** dissolved in chloroform were deposited on the ITO-covered glass plate. Later, the thin film

is annealed at 80 °C for 25 minutes. Next, silver contacts were deposited onto the thin layer using a sputtering process. Memory characterization was carried out at room temperature with a Keithley 4200A semiconductor parameter analyzer. **Figure S35** shows the schematic representation of the fabricated device.

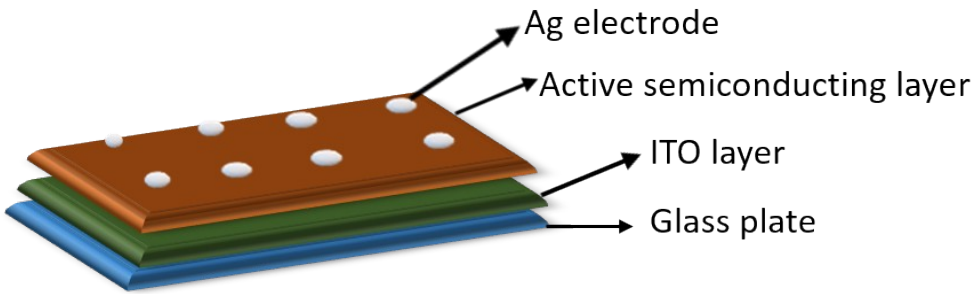

Figure S35: Memory devices fabrication of the synthesized molecules

References

1. Frisch, M. J.; Trucks, G. W.; Schlegel, H. B.; Scuseria, G. E.; Robb, M. A.; Cheeseman, J. R.; Scalmani, G.; Barone, V.; Mennucci, B.; Petersson, G. A.; Nakatsuji, H.; Caricato, M.; Li, X.; Hratchian, H. P.; Izmaylov, A. F.; Bloino, J.; Zheng, G.; Sonnenberg, J. L.; Hada, M.; Ehara, M.; Toyota, K.; Fukuda, R.; Hasegawa, J.; Ishida, M.; Nakajima, T.; Honda, Y.; Kitao, O.; Nakai, H.; Vreven, T.; Montgomery, J. A.; Peralta, J. E.; Ogliaro, F.; Bearpark, M.; Heyd, J. J.; Brothers, E.; Kudin, K. N.; Staroverov, V. N.; Kobayashi, R.; Normand, J.; Raghavachari, K.; Rendell, A.; Burant, J. C.; Iyengar, S. S.; Tomasi, J.; Cossi, M.; Rega, N.; Millam, N. J.; Klene, M.; Knox, J. E.; Cross, J. B.; Bakken, V.; Adamo, C.; Jaramillo, J.; Gomperts, R.; Stratmann, R. E.; Yazyev, O.; Austin, A. J.; Cammi, R.; Pomelli, C.; Ochterski, J. W.; Martin, R. L.; Morokuma, K.; Zakrzewski, V. G.; Voth, G. A.; Salvador, P.; Dannenberg, J. J.; Dapprich, S.; Daniels, A. D.; Farkas, O.; Foresman, J. B.; Ortiz, J. V.; Cioslowski, J.; Fox, D. J.. Gaussian 09, revision A.1; Gaussian, Inc.: Wallingford, CT, 200